AALBORG UNIVERSITY

DENMARK

Delamination in composites with fiber bridging under quasi-static loading and variable amplitude fatigue loading

Mosbjerg Jensen, Simon

[Link to publication from Aalborg University](#)

DELAMINATION IN COMPOSITES WITH FIBER BRIDGING UNDER QUASI-STATIC LOADING AND VARIABLE AMPLITUDE FATIGUE LOADING

BY
SIMON MOSBJERG JENSEN

DISSERTATION SUBMITTED 2021

AALBORG UNIVERSITY
DENMARK

Delamination in composites with fiber bridging under quasi-static loading and variable amplitude fatigue loading

Simon Mosbjerg Jensen

Department of Materials and Production
Solid and Computational Mechanics Research Group
Aalborg University, Denmark

PhD Thesis
2021

Preface

This thesis has been submitted to the Faculty of Engineering and Science at Aalborg University in partial fulfilment of the requirements for the degree of Doctor of Philosophy in Mechanical Engineering. The work has been carried out at the Department of Materials and Production at Aalborg University during the period from April 2018 to March 2021. This includes a research stay abroad at the research group AMADE (Analysis and Advanced Materials for Structural Design) at the University of Girona, Spain from October to December 2020.

Reader's guide

The primary work conducted during the PhD study has been reported in four journal papers. The thesis is written as an article-based thesis, which consists of an extended summary and a number of individual journal papers published independently of each other. The journal papers are appended this document and have been reprinted to fit the format of this thesis with permission.

In Chap. 1 *Introduction*, the topic of delamination in laminated fibre reinforced composite structures is introduced and motivated. The chapter introduces basic concepts and analysis tools/methods that will be treated in the current work, and provides the basic justification of the research focus. Some of the topics covered in Chap. 1 will be revisited in Chap. 2 at a higher level of detail. Readers already familiar with the topic may go through Chap. 1 casually, but are encouraged to visit Sec. 1.6, which provides a description of the project objectives. Chap. 2 *State-of-the-Art Literature Review* covers a review of the relevant scientific publications in the literature to identify the novelty and relevance of the work conducted in the project. Finally, Chap. 3 *Summary of Papers* gives a brief summary of the four journal papers and highlights the papers' contribution and impact. The journal papers are included in appendix.

Acknowledgements

Several persons have been helpful to me throughout this Ph.D. project, whether it is due to learning of scientific topics, practical matters, or to stay motivated when the project at times has appeared to go one step forward and two steps back.

A special thanks goes to my supervisors Associate Professor Esben Lindgaard and Associate Professor Brian Lau Verndal Bak, who have made it possible for me to conduct the present research. I have appreciated their competent and well-balanced guidance, support, and general enthusiasm in every detail of the project.

I would also like to thank all the members of the CraCS Research Group, which have been my daily office mates, and have provided excellent frames for instructive technical discussions. I would also like to thank my friend and former fellow student Mario Javier Martos Sánchez for his support and contribution in papers A and B.

During the project I visited the research group AMADE at the University of Girona from October to December 2020. I would like to express my sincere gratitude to Associate Professor Jordi Renart for hosting my external research stay, for the many interesting technical discussions, and for giving me the opportunity to get insight and participate in an international research environment - despite the challenges and lock-downs caused by Covid19. I look forward to continue and finalise the work that we conducted during this period.

Thanks to the colleagues in the Solid and Computational Mechanics Research Group at Aalborg University for an enjoyable and inspiring research and teaching environment. Finally, many of the experimental tests conducted as part of this project could not be realised without the support from technicians and engineers at the laboratory of the Department of Materials and Production. Thank you for your help and expertise in manufacturing and machining of test specimens and components for various test fixtures.

Aalborg, April 2021

Simon Mosbjerg Jensen

Contents

Abstract

Failure of laminated fibre-reinforced composite structures is often caused by propagation of delaminations (interlaminar cracks) due to the relatively weak interlaminar strength. To obtain innovative design solutions of advanced composite structures a damage tolerant design approach is often a prerequisite, such that structures are designed to maintain their functionality despite the presence of damage. This requires advanced simulation tools and a thorough understanding of the progression of delaminations under static and fatigue loading to ensure that sub-critical cracks will not grow to critical sizes between periodic inspections. Firstly, the work in this thesis deals with numerical models and characterisation methods in a cohesive zone modelling framework to simulate delamination under quasi-static loading. Secondly, experimental testing campaigns are carried out to understand and characterise fatigue-driven delamination growth and governing damage mechanisms under variable amplitude loading.

The thesis is based on four journal papers A-D. In paper A a new multi-linear mixed-mode cohesive law is developed to be able to simulate quasi-static delamination with a complex fracture process zone due to large-scale fibre bridging. In paper B a robust and efficient method is developed to characterise advanced parametric cohesive laws using inverse parameter identification and gradient-based optimisation. The models and methods in paper A-B provide an accurate representation of cohesive tractions and the simulated results are shown to be in good agreement with experimental measurements.

Papers C-D investigate fatigue-driven delamination under variable amplitude loading. This is motivated by a need to improve the understanding of fatigue-driven delamination under real load spectra (i.e. in-service loads), which are far from the highly idealised constant amplitude loading conditions applied to test specimens for characterisation of fatigue properties and model parameters. The conventional double cantilever beam specimen (DCB) test is applied in paper C to investigate the crack growth behaviour following a single step change in load amplitude under different load sequences in comparison to base-line data obtained under constant amplitude loading. In paper D, the crack growth behaviour due to variable amplitude load patterns with multiple load amplitude changes are studied in a G-controlled cyclic test using the pure moment loaded DCB test configuration. The studies identify

characteristic load interaction effects that increase the crack growth rate significantly - especially when frequent load amplitude changes occur. In spite of this, load interaction effects are neglected in state-of-the-art delamination prediction models and the errors introduced by such assumptions are currently unknown.

Dansk Resumé

Delaminering er ofte den primære årsag til brud i laminerede fiberforstærkede plast kompositter på grund af deres relativt lave interlaminære styrkeegenskaber. En skadestolerant designfilosofi er ofte nødvendig for at kunne udvikle innovative designløsninger af kompositstrukturer, således at strukturerne kan opretholde deres funktion på trods af tilstedeværelsen af skade. Dette kræver avancerede simuleringsværktøjer samt en grundig forståelse af revnevækst under statisk belastning og udmattelse for at sikre at sub-kritiske revner ikke vil vokse til en kritisk størrelse imellem periodiske inspektioner. Det videnskabelige arbejde i denne afhandling omhandler to primære temaer inden for delaminering i fiberforstærkede plast kompositter. For det første udvikles numeriske modeller og karakteriseringsmetoder indenfor kohæsiv zone modellering til simulering af revnevækst under kvasi-statisk belastning. For det andet udvikles og udføres eksperimentelle testkampagner for at forstå og karakterisere revnevækst (delaminering) samt underliggende skadesmekanismer under påvirkning af cyklisk varierende belastninger med variabel amplitude.

Afhandlingen er baseret på fire videnskabelige artikler A-D. I artikel A udvikles en ny multi-lineær kohæsiv lov til simulering af mixed-mode kvasistatisk delaminering med en kompleks brudproces zone som følge af krydsende fibre bag revnespidsen. I artikel B udvikles en robust og effektiv metode til karakterisering af avanceret parametriske kohæsive love ved brug af invers parameter-identifikation og gradient-baseret optimering. Modellerne og metoderne i artiklerne A-B viser en nøjagtig repræsentation af kohæsive spændinger og de simulerede responskurver er i god overensstemmelse med eksperimentelle målinger.

I artiklerne C-D undersøges udmattelse under variabel amplitude belastning. Dette motiveres af et behov for at opnå en bedre forståelse af revnevækst under påvirkning af virkelige belastningsspektre (in-service belastningsspektre), som er markant forskellige fra de yderst idealiseret konstant amplitude belastninger der påføres testemner når udmattelsesegenskaber og model parametre karakteriseres. Den konventionelle DCB (double cantilever beam) test anvendes i artikel C til at undersøge revnevækstopførelsen efter et enkelt skift i belastningsamplitude under forskellige last sekvenser til sammenligning med referencemålinger fra konstant amplitude test. I artikel D studeres revnevækstopførelsen i løbet af belastningsspektre som indeholder flere på

hinanden følgende last amplitude skift. I artikel D anvendes DCB emner påført rent bøjningsmoment til G-kontrolleret udmattelsesprøvning. Studierne i artiklerne C-D identificerer karakteristiske last-interaktionseffekter som øger revnevækstraten markant – særligt når hyppige last amplitude skift forekommer. På trods heraf, negligeres last-interaktionseffekter i state-of-the-art modeller til simulering af delaminering og fejlen introduceret herved er endnu uvis.

Publications and Conferences

The thesis is written as an article-based thesis, which consists of an extended summary four journal papers. The following contains a list of the publications produced and the conferences attended during the PhD study.

Publications in Journals

A) Jensen SM, Martos MJ, Bak BLV & Lindgaard E (2019) Formulation of a mixed-mode multilinear cohesive zone law in an interface finite element for modelling delamination with R-curve effects. *Composite Structures*, 216: 477-486. doi:https://doi.org/10.1016/j.compstruct.2019.02.029.

B) Jensen SM, Martos MJ, Lindgaard E & Bak BLV (2019) Inverse parameter identification of n-segmented multilinear cohesive laws using parametric finite element modelling. *Composite Structures*, 225: 111074. doi:https://doi.org/10.1016/j.compstruct.2019.111074.

C) Jensen SM, Bak BLV & Lindgaard E (2021) Transition-behaviours in fatigue-driven delamination of GFRP laminates following step changes in block amplitude loading, *International Journal of Fatigue*, 144: 106045. doi:https://doi.org/10.1016/j.ijfatigue.2020.106045.

D) Jensen SM, Bak BLV, Bender JJ, Carreras L & Lindgaard E (2021) Transient delamination growth in GFRP laminates with fiber bridging under variable amplitude loading in G-control, *submitted for review*.

Publications in Proceedings

E) Jensen SM, Martos MJ, Bak BLV & Lindgaard E (2018) Identification of a novel cohesive zone law in an interface finite element for simulating delamination with R-curve effects. In: *Proc. of ECCM 2018 - 18th European Conference on Composite Materials*. Athens, Greece, 24-28 June: 7 s.

Conferences and symposia

The conferences and symposia attended during the PhD study with an oral presentation are listed in the bullets below.

F) Jensen SM, Martos MJ, Bak BLV & Lindgaard E (2018) Identification of a novel cohesive zone law in an interface finite element for simulating delamination with R-curve effects. *ECCM 2018 - 18th European Conference on Composite Materials*. Athens, Greece, 24-28 June.

G) Jensen SM, Bak BLV & Lindgaard E (2019) Fatigue-driven delamination in laminated composite structures considering real load spectra. *DCAMM Symposium 2019*. Vejle, Denmark, 11-13 March.

H) Jensen SM, Martos MJ, Bak BLV & Lindgaard E (2019) A mixed-mode multi-linear cohesive law: Numerical formulation, model identification and delamination with R-curve behaviour. *7th ECCOMAS Thematic Conference on the Mechanical Response of Composites: COMPOSITES 2019*. Girona, Spain, 18-20 September.

I) Jensen SM, Bak BLV, Bender JJ, Carreras L & Lindgaard E (2021) Fatigue-driven delamination in GFRP laminates under variable amplitude loading and G-control cyclic testing. *AMADE Day Winter 2021, University of Girona*. Virtual mini-symposium, January 26.

1

Introduction

This thesis deals with delamination in laminated fibre-reinforced composite materials. The scope of the project is to develop models and characterisation methods to simulate quasi-static delamination, and to understand fatigue-driven delamination and underlying mechanisms under variable amplitude loading. Models and characterisation methods are developed in the cohesive zone model framework for quasi-static loading. Experimental testing is conducted on coupon level using fracture mechanical test specimens subjected to variable amplitude loading. Special attention is given to load interaction effects, which are inevitable in fatigue under real load spectra.

This chapter presents a rather coarse introduction to basic concepts and the theoretical background of the topics covered in the scientific papers A-D. Several of the topics are revisited at a higher level of detail in the next chapter on state-of-the-art within selected topics. The first section introduces laminated fibre-reinforced polymer composite structures and damage tolerant designs. Delamination and considerations of large-scale fracture process zones are explained in Sec. 1.2-1.3. In Sec. 1.4 basic concepts of the cohesive zone model are addressed. Fatigue-driven delamination, real load spectra, and load interaction effects are introduced in Sec. 1.5. Finally, the objectives of the project are specified in Sec. 1.6.

1.1 Laminated composite structures

Laminated fibre-reinforced composite materials are ideal for many structural applications due to two major advantages, among many others. Firstly, laminated fibre-reinforced composite materials have high strength-to-weight and stiffness-to-weight ratios which make these materials specially suited for weight-sensitive structural applications. Secondly, the fibre-reinforced composite materials allow tailoring of material properties to meet a particular structural requirement with little waste of material capability (Jones, 1999).
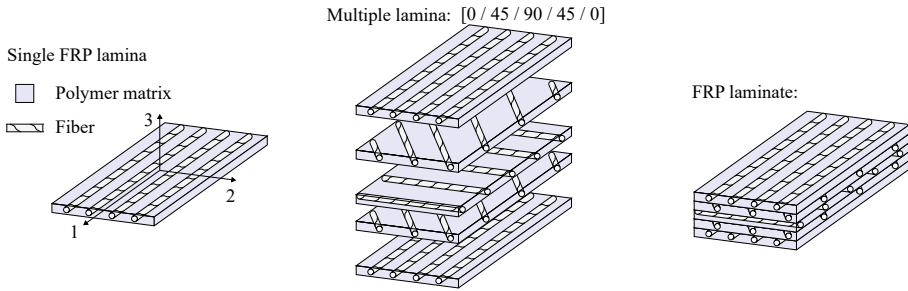
Fig. 1.1: A fibre-reinforced composite with polymer matrix and continuous fibres. A laminated fibre-reinforced polymer (FRP) composite is shown to the right in a $[0°/45°/90°/45°/0°]$ layer stacking configuration.

Perfect tailoring of a composite material provides only the stiffness and strength required in each direction. These properties explain the wide application of fibre-reinforced composite materials, for example in wind turbine blades, naval industries, and sports equipment such as kayak monocoques. In the following, a brief introduction is given to laminated fibre-reinforced composite materials and damage in laminated composite structures. Finally, a wind turbine blade is used to exemplify some of the key concepts discussed throughout this section and provide a contextual background for the research topic as a whole.

1.1.1   Laminated fibre-reinforced composite materials

A composite material is a type of material in which two or more materials are combined on a macroscopic scale. The composite material exhibits a significant proportion of the properties of both constituent materials such that a better combination of properties is realised. The composite materials under consideration in the current work are fibre-reinforced composite materials with a polymer-matrix and continuous fibres, as illustrated in Fig. 1.1. Typically, the matrix is of considerably lower density, stiffness and strength than the small diameter fibres of high stiffness and strength. The polymer-matrix binds the fibres together, acts as a protecting medium, and transfers the externally applied stress to the fibres; only a very small portion of the applied load is sustained by the matrix (Jones, 1999). Generally, fibre reinforced polymer (FRP) composite materials possess anisotropic materials properties. FRP composite materials have a large strength and stiffness in the fibre direction (e.g. direction 1 in Fig. 1.1), but possess relatively low values of the corresponding properties in the direction perpendicular to the fibre axis (e.g. direction 2 in the single FRP lamina in Fig. 1.1), where basically, loads are carried by the matrix (Jones, 1999).

Laminated FRP composite materials consist of multiple fibre-layers, also

know as lamina, of potentially different orientation in a stacking configuration as illustrated in Fig. 1.1, which are bonded together to act as an integral structural element. The orientation, layer thickness and stacking sequence may be tailored to a given structural application, for example the fibre orientations may be aligned with respect to the principal stress directions.

The complex and manifold architecture of laminated FRP composite materials yields a wide range of failure mechanisms, which may operate at different length scales. For example, fibre-matrix debonding occurs at a microscopic scale while matrix cracking and interlaminar cracking occurs at a macroscopic scale (Talreja and Varna, 2016). During a fracture process, several failure mechanisms usually co-exist and may interact with each other. Additionally, the fracture process and the governing failure mechanisms are dependent on the applied load level. These basic considerations make fracture analysis of FRP composite materials challenging.

1.1.2 Damage tolerant design

It requires a damage tolerant design philosophy to include considerations on damage initiation and propagation in the design process. The damage tolerant design philosophy accepts that a distribution of damage locations can exist within a structure. The design philosophy is different from the conventional safe-design approach. The safe-design philosophy is typically based on experience from previous designs and the first principles of composite mechanics, which prevents innovative designs, leads to unnecessary large factors of safety, and underestimation of the actual material properties (Jensen and Fugleberg, 2015). The damage tolerant design approach requires advanced techniques and computational tools, by contrast, that allows to predict damage onset and growth in order to verify that sub-critical damage will not grow to critical sizes between periodic inspections. The development of computational methods for damage tolerant design is still a problem under investigation - particularly as new materials emerge with complex damage processes. Such computational methods will be treated in later sections. An example of a modern laminated FRP composite structure and damage tolerant design considerations are introduced next.

Example: Large damage tolerant wind turbine blades

Fracture in laminated FRP composite structures and the damage tolerant design approach are put in an industrial and societal context by this brief example. The world population, wealth, CO_2 emissions, and the global temperature are four very closely related and increasing global phenomena in the 21st century (United Nations, 2019; Djursing, 2021). One major challenge is to
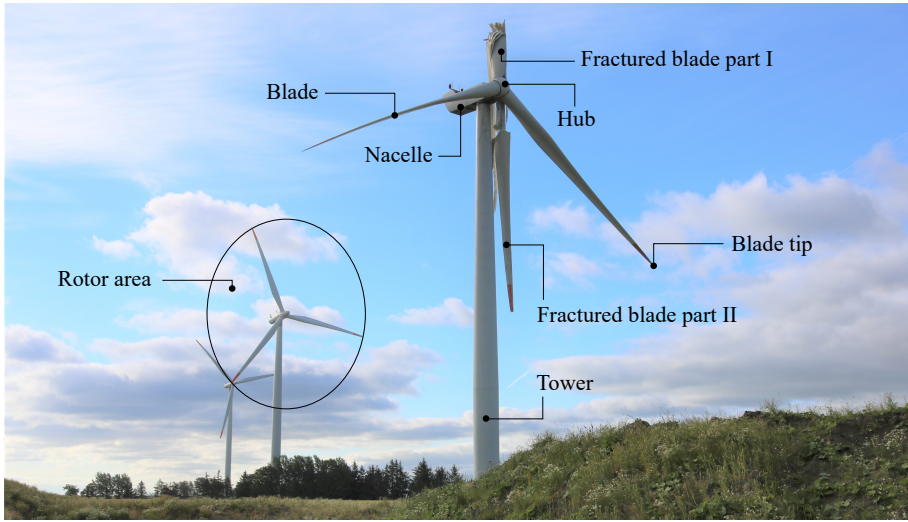
(a)
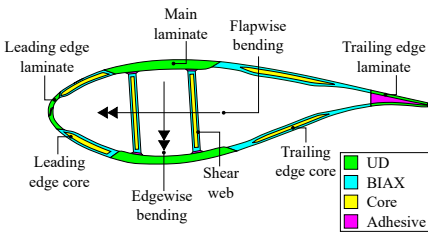
(b)
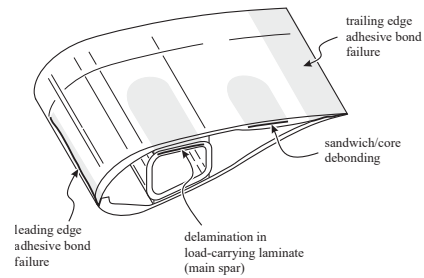
(c)

Fig. 1.2: (a) A fractured blade on the front wind turbine. Rotor diameter: 92 m, hub-height: 70 m. The wind turbine is installed in the late 90s, image taken July 2020. (b) A typical cross-section of a wind turbine blade. (c) Schematic of major failure modes in sub-structure of a wind turbine blade. The shaded areas indicate cracked internal regions. Reprinted from (McGugan et al., 2015) with permission from publisher Royal Society ©.

reduce the CO_2 emission of modern societies to a level that step-by-step can be shared by 10-11 billion people by the end of this century (Rosling, 2013; United Nations, 2019). Renewable energy sources are vital in this regard to decarbonise the current energy production systems and processes.

According to the central scenario in a recent report from a European wind energy association, the wind energy will be able to produce 888 TWh in Europe by 2030, which is equivalent to 30% of the EU's power demand (Nghiem and Pineda, 2017). Even higher wind energy shares are possible; in 2020, approximately 48% of Denmark's total demanded electricity was covered by wind energy (WindEurope, 2021).

One of the effective ways of optimising the power output of wind turbines, is to increase the length of the wind turbine blades. Especially, in the off-shore wind turbine industry, where the recently launched 15 MW wind turbine V236-15.0MW has a blade length of 115.5 m (Wittrup, 2021; Vestas, 2021). However, increasing the length of the wind turbine blade adds significant weight to the structure (Mikkelsen, 2016), and inevitable manufacturing defects increase in number as the volume of the blade increases. The manufacturing defects are likely to initiate damage that may grow in size over time and cause fracture of the wind turbine before the design lifetime is met, as shown by example in Fig. 1.2(a). Damage tolerant design approaches and damage tolerant materials, e.g. materials that possess increasing fracture resistance with increasing damage size/crack extension, are highly suited in this regard in order to prevent a given defect from reaching a critical size (McGugan et al., 2015).

Two important prerequisites for application of damage tolerant concepts is advanced numerical models to predict the residual life of the damaged blade, and a thorough understanding of governing failure modes in the blade. Several failure modes can occur in wind turbine blades. A schematic outline of a typical cross section of a wind turbine blade is provided in Fig. 1.2(b), which also highlights the dominant FRP laminates in different regions of the cross section. The main laminates in Fig. 1.2(b) are the primary load carrying components of the blade which sustain the aerodynamic loads causing flapwise bending of the blade. The main laminates primarily consist of unidirectional (UD) laminates with the fibre direction aligned with the longitudinal direction of the blade. Some of the major macroscopic failure modes in wind turbine blades are reported in Fig. 1.2(c) (Sørensen et al., 2004). The delaminations in the main laminate is one of the most important failure modes in this regard.

1.2 Delaminations in FRP laminates

1.2.1 Interlaminar cracking

Delamination growth is an interlaminar cracking process in laminated composite materials, in which a crack propagates along the interface of neighbouring layers. A delamination crack in a UD laminate is exemplified in Fig. 1.3 at the interface of layer 3 and layer 4. Delamination is one of the most common damage mechanisms in laminated FRP composite materials due to their relatively weak interlaminar strength, and is probably the most troublesome damage mechanism for composite designers. Delaminations may originate in FRP laminates for several reasons (Jones, 1999; Pagano and Schoeppner, 2000; Millán and Armendáriz, 2015), for example, due to design features prone to

develop interlaminar stresses (e.g. free edges whether they be at the edge of a plate or around a hole), manufacturing defects (air pockets, resin-rich pockets, wrinkles, and matrix shrinkage during curing), and environmental effects such as temperature and moisture. Transverse concentrated loads caused by low velocity impacts are also likely to initiate delamination. In fatigue loading, delaminations are often a secondary damage mechanism which have initiated from intralaminar damage sites such as transverse matrix cracks (Gamstedt and Sjögren, 2002; Talreja and Varna, 2016). Generally, delaminations reduce the structure's load carrying capacity and degrade the structural properties. Moreover, delaminations are prone to propagate when compression and out-of-plane loads (static and fatigue) are applied to the structure which eventually may lead to structural collapse (Millán and Armendáriz, 2015).

The three basic opening modes of a crack is shown in Fig. 1.4. Cracks in homogeneous isotropic materials tend to grow under mode I. However, interlaminar cracks in laminated FRP composite materials are often constrained to propagate along the relatively weak layer interfaces (Sørensen, 2016). The external load configurations and bi-material interfaces make delaminations prone to propagate under mixed-mode conditions.

1.2.2 Fibre bridging and fracture process zone

The growth of an interlaminar crack involves formation of damage in the vicinity of the crack tip. The underlying damage processes are manifold, and depend on the material system and the local state of stress (mode I, mode II, mode III and mixed-mode). A schematic illustration of damage processes in the vicinity of a macroscopic interlaminar crack is provided in Fig. 1.3. A damage zone ahead of the macroscopic crack tip is typically formed, which contains plastic deformation and microcracks whose coalescence and
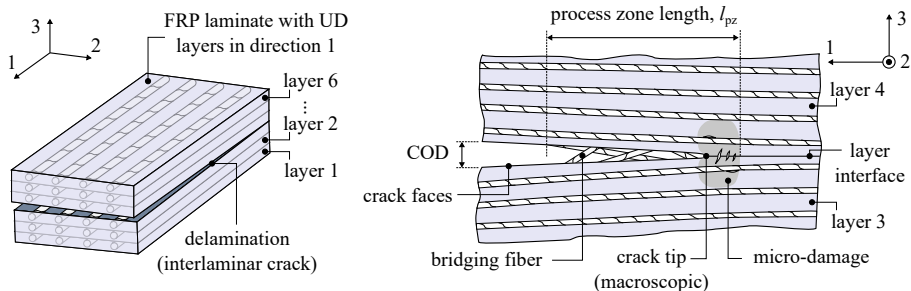

Fig. 1.3: Schematic outline of a delamination in a UD 0° laminate. The material in the vicinity of the crack tip is illustrated to the right in the figure. The damage zone ahead of the macroscopic crack tip involves plastic deformation and matrix microcracking. Fibres bridge the crack faces in the wake of the macroscopic crack tip.
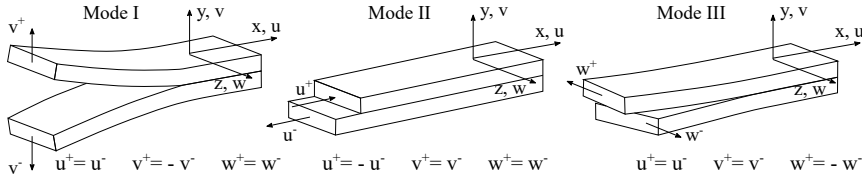
Fig. 1.4: Pure crack opening modes and corresponding crack opening displacement components of the upper $(+)$ and lower $(-)$ crack faces.

growth results in extension of the macroscopic crack. Interlaminar cracking in FRP laminates is certainly a matrix-dominated fracture process, however, some interaction with the fibres are inevitable because of local crack path instability and imperfect fibre alignments (Whitney, 1989; Hwang and Han, 1989; Hashemi et al., 1990b; Spearing and Evans, 1992). In continuous FRP laminates obtained by stacking of UD layers, fibres commonly bridge the crack faces in the wake of the macroscopic crack tip, as illustrated in Fig. 1.3. This phenomenon is commonly known as cross-over fibre bridging (Hashemi et al., 1990b; Spearing and Evans, 1992; Suo et al., 1992; Bao and Suo, 1992; Sørensen and Jacobsen, 2000).

Cross-over fibre bridging is characterised by a relatively low traction ~ 1 MPa operating over a large crack opening displacement (COD) ~ 1 mm (Suo et al., 1992; Bao and Suo, 1992; Sørensen and Jacobsen, 2000) (even up to COD ≈ 10 mm in glass/epoxy laminates), which results in a large fibre bridging zone in the wake of the crack tip. The length of the fibre bridging zone is typically comparable to, or larger than, the thickness of the laminate, which is commonly known as large-scale fibre bridging. The density of bridging fibres is usually highest near the crack tip and decreases throughout the crack wake as the distance from the crack tip increases. The fibre bridging zone shields the crack tip and thereby enhances the fracture resistance of the material.

The term fracture process zone (FPZ) is used to denote the region wherein material degradation occurs. Thus, the FPZ includes micro-damage mechanisms ahead of the macroscopic crack tip and bridging fibres in the crack wake as illustrated by the FPZ length, l_{pz}, in Fig. 1.3.

1.3 Large-scale fracture process zones

1.3.1 K-dominant zone

Fracture mechanics considerations are fundamental to characterise and model delamination growth. The objective of linear elastic fracture mechanics (LEFM) is to analyse the load carrying capacity of a component before a pre-existing crack will start to grow. The LEFM approach relies on continuum mechanics

solutions of stress intensity factors (SIF). Assumptions of LEFM are that the material behaves linear-elastic, deformations are small (i.e. small displacements and small strains are assumed), and the elastic field in a component is analysed as if the crack tip is a mathematical point (2D) with no spatial extent i.e. the FPZ is neglected (Sun and Jin, 2012; Bao and Suo, 1992; Sørensen, 2016). The stress field in the vicinity of the crack tip (the near-tip stress field) is square root singular as shown in Eq. (1.1)[1] for a mode I crack.

$$\sigma_{ij} \approx \frac{K_I}{(2\pi r)^{1/2}} f_{ij}^I(\theta) \quad (1.1)$$
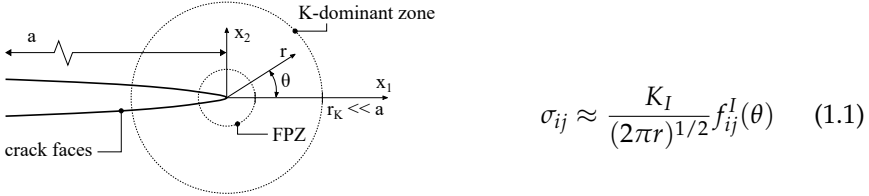
Fig. 1.5: K-dominant zone and small-scale fracture process zone (FPZ) in isotropic solid.

where r and θ are the polar coordinates centred at the crack tip as shown in Fig. 1.5, the functions $f_{ij}^I(\theta)$ are universal trigonometric functions of θ (available in elasticity textbooks, e.g. (Sun and Jin, 2012; Zehnder, 2012) or (Rice, 1968)), and K_I is the mode I SIF. According to LEFM the singular near-tip stress field in Eq. 1.1 is universal and applies to any cracked component of arbitrary geometry and external boundary conditions undergoing mode I cracking. Accordingly, the SIF is the only quantity that determines the magnitude of the (universal) stress field in the vicinity of the crack tip, and hence the only quantity which connects the structure's geometry and external boundary conditions to the crack process. In real materials, the actual stress field will not be singular and stresses will redistribute at the crack tip within an inelastic FPZ of a certain length l_{pz}. If the size of the FPZ is much smaller than the macroscopic crack length as well as relevant structural dimensions, i.e. the material is elastic over the entire structure except from a small zone localised at the crack tip, a small-scale FPZ condition prevails. Under small-scale FPZ conditions, the near-tip stress field is well approximated by the solutions in Eq. 1.1 within an annulus near the crack tip ($r > l_{pz}$ and $r << a$), and the crack process can be described by the single scalar parameter, K_I.

Therefore, the resistance to fracture can be defined as the maximum SIF that a material can sustain. In practice, for a given cracked component made of a certain material, the crack will grow if: $K \geq K_c$, where K denotes the SIF of the given geometry and external boundary conditions, and K_c the critical SIF of the given material.

---

[1]this is the first dominant term of a Taylor expansion of a complete solution. However, close to the crack tip, higher order terms vanish and the singular term dominate.
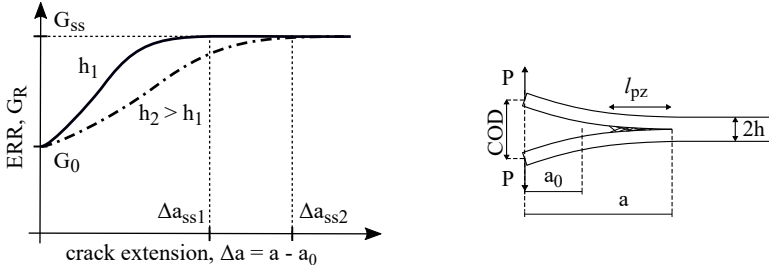
Fig. 1.6: R-curve in case of large-scale fibre bridging. Notice, the length of the FPZ, l_{pz}, is comparable to the specimen thickness, h. The shape of the R-curve depends on the height ($h_2 > h_1$).

Many fracture problems violate the small-scale FPZ condition and it becomes necessary to distinguish between small- and large-scale FPZs. Large-scale FPZs are common in delamination analysis of laminated FRP composite materials due to large-scale fibre bridging as explained in Sec. 1.2.2. In a fracture mechanics sense, a large-scale FPZ imply that damage processes outside the K-dominant zone influence the damage process at the crack tip, and the SIF, K, looses its property as the only quantity that connects the geometry and external boundary conditions to the crack process. Consequently, the single-parameter framework in classical LEFM becomes invalid, and alternative approaches are necessary to determine the load carrying capacity of a cracked component (Bao and Suo, 1992).

The basic fracture mechanics concepts introduced in this section applies directly to homogeneous isotropic materials. The fracture mechanics analysis of an orthotropic material is more complicated, however, the crack tip stress field still possess a square-root singularity (Sih et al., 1965; Sørensen, 2016). Additionally, further complexities is added when cracks grow between elastic dissimilar materials, e.g. delaminations between layers of different fibre orientation, which may cause oscillatory stress singularities (Hutchinson and Suo, 1992; Sørensen, 2016). Nevertheless, such details are outside the scope of the current section.

1.3.2 R-curves and bridging laws

It is well-established that fibre bridging can enhance the fracture resistance during crack growth in laminated FRP composite materials. The rising fracture resistance is typically characterised by a resistance curve (R-curve). The R-curve is typically described in terms of the crack extension, Δa versus the energy release rate (ERR), G_R, required to propagate the crack, as illustrated in Fig. 1.6. To obtain the R-curve, an artificial pre-crack of length a_0 is made prior to the fracture test. Upon loading, a crack tip driving force, G_0, which

is approximately equal to the critical ERR of the matrix, extends the crack. As the crack length, a, increases and more fibres bridge the crack faces, a higher ERR, G_R, is needed to maintain the crack growth, which causes the rising R-curve (Bao and Suo, 1992). When the crack reaches a certain crack extension, Δa_{ss}, the FPZ will translate along with the macroscopic crack tip, cracking the matrix in the front and breaking bridging fibres in the wake. The characteristic quantities of an R-curve are the initiation ERR, G_0, the plateau ERR, G_{ss}, and the crack extension, Δa_{ss}, to attain the plateau level.

For small-scale FPZ conditions the R-curve can be regarded as a material property. However, under large-scale FPZ conditions the shape of the R-curve is no longer a material property as it depends on the specimen geometry, as indicated in Fig. 1.6 (Spearing and Evans, 1992; Suo et al., 1992; Bao and Suo, 1992; Sørensen and Jacobsen, 1998).

In Fig. 1.6 the plateau ERR, G_{ss}, is assumed to be independent of the specimen thickness, h. This is consistent with some experimental studies in the literature. For example the investigation of quasi-static delamination in unidirectional laminated carbon/epoxy composites in (Sørensen and Jacobsen, 1998). However, other studies show a specimen thickness dependency on the plateau ERR, G_{ss}, e.g. (Farmand-Ashtiani et al., 2014) who investigated R-curves in a similar material system.

Traction-separation relations, or so-called bridging laws (Suo et al., 1992; Bao and Suo, 1992), can also be used to characterise large-scale fibre bridging. The bridging law is a homogenized nonlinear traction-separation law that gives a relationship between the local COD and the local traction on the crack faces caused by the bridging ligaments. As before, there are different opinions in the literature on the bridging laws' dependency of the specimen geometry; some studies show that the bridging law is independent of the specimen geometry (i.e. a material property) (Sørensen and Jacobsen, 1998) whereas other studies show that the bridging law depends on the specimen geometry (Farmand-Ashtiani et al., 2014).

The bridging laws may be measured experimentally, for example (Sørensen and Jacobsen, 1998; Farmand-Ashtiani et al., 2014), or may be derived from micro-mechanical models (Spearing and Evans, 1992; Kaute et al., 1993; Albertsen et al., 1995; Ivens et al., 1995; Sørensen and Jacobsen, 1998; Soerensen et al., 2008; Daneshjoo et al., 2018; Grytten et al., 2020). For example, the bridging laws derived from micro-mechanical models in (Spearing and Evans, 1992; Sørensen et al., 2008) show that bridging tractions are inversely proportional to the square root of the COD under mode I crack opening (if shear deformation in the bridging ligament is neglected).

Similar traction-separation relations will be considered in later sections on cohesive zone modelling, and experimental characterisation of traction-separation relations are considered in Sec. 2.1.3.

1.4 Computational methods to delamination

1.4.1 Two major approaches

Crack propagation is in nature a nonlinear problem and requires numerical solution methods, which in all practical applications involve implementation in the finite element method (FEM) framework. There are two major approaches to numerical simulation of delamination. The first category is based on direct application of LEFM and the second category is based on a cohesive zone model (CZM) (Bak et al., 2014).

When the basic assumptions of LEFM applies, see Sec. 1.3.1, methods based on direct application of LEFM have proven to be effective in predicting delamination growth. An example includes the virtual crack closure technique (VCCT) (Rybicki and Kanninen, 1977; Krueger, 2002, 2011; Bak et al., 2014), which is based on the assumption that when a crack extends by a small amount, the energy released in the process is equal to the work required to close the crack to its original length. However, the small-scale FPZ assumption of LEFM limits the application of these methods for prediction of delamination in laminated FRP composite materials due to large-scale fibre bridging. Additionally, the LEFM methods, e.g. the VCCT method, cannot predict crack initiation (a pre-existing crack is required), and the methods are not suited for bi-material interfaces.

The cohesive zone model (CZM) is an approach to adopt inelastic behaviour in materials near the crack tip with the intention of describing more realistic material separation mechanisms and avoid the crack tip stress singularity (Sun and Jin, 2012). The CZM adds a cohesive zone near the crack tip, in which the crack faces are held together by a cohesive traction. The separation process is described by a traction-separation relation between the cohesive traction and the opening displacement of the crack faces. The traction-separation relation is known as the cohesive law (Sun and Jin, 2012). Eventually, the opening displacement at the tail of the cohesive zone will reach a critical value causing zero tractions at this location, which represents complete material failure. Conceptually, the CZM combines damage mechanics and fracture mechanics frameworks; the CZM has an intrinsic fracture energy dissipating mechanism, the CZM can predict both delamination initiation and propagation, and the CZM is not limited to small-scale FPZ conditions. These considerations make the CZM favourable to study delamination in laminated FRP composite materials. Further details on CZM will be given in the following sections.
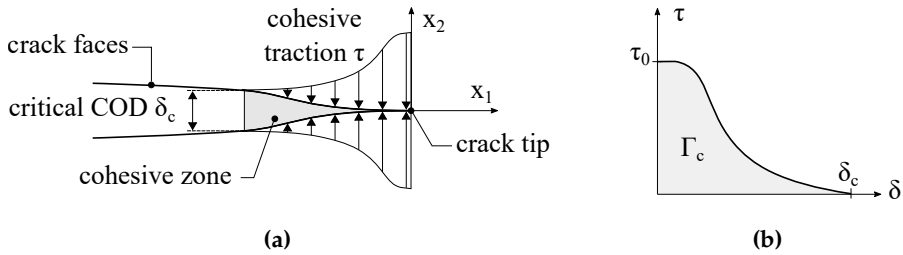
Fig. 1.7: (a) Cohesive zone near the crack tip. (b) Generic cohesive law.

1.4.2 Basic concepts in cohesive zone models

The origin of the cohesive zone concept is often attributed to the independent work by Barenblatt (Barenblatt, 1959, 1962) and Dugdale (Dugdale, 1960), who both assumed finite stresses at the crack tip and introduced a traction field acting on the crack faces as illustrated in Fig. 1.7(a). In order to propagate the crack, these tractions must be overcome by an outer applied load. Barenblatt considered the crack face separation mechanism at the atomic scale and described the cohesive tractions as a result of atomic bonding forces. Dugdale assumed that the cohesive tractions are due to perfect plastic behaviour within a yield strip in the wake of the crack tip. Considerations on the underlying separation mechanism is a prominent feature of the CZM in comparison to LEFM. Since the pioneering work in (Barenblatt, 1959, 1962; Dugdale, 1960) the cohesive zone concept has been further refined and adopted to new material systems. This has also given rise to many physical interpretations of the various mechanisms responsible for cohesive tractions in cracking processes. For example, CZMs of delamination in laminated FRP composite materials typically involve cohesive tractions due to crack tip micro-cracking, small-scale yielding, and fibre bridging in the crack wake.

Hillerborg (Hillerborg et al., 1976) originally extended the cohesive zone concept in (Barenblatt, 1959, 1962), which was limited to propagation of pre-existing cracks, to incorporate a crack formation criterion. Considerations from strength of materials are combined with the cohesive zone concept, and damage is proposed to initiate at an arbitrary location when the stress reaches the tensile strength of the material (Hillerborg et al., 1976). Similar considerations are applied in modern CZM such that a damage initiation criterion and a propagation criterion are unified in the cohesive law.

Cohesive law and energy dissipation

The cohesive tractions, τ, are related to the crack opening displacement, δ, through the cohesive law as exemplified in Fig. 1.7(b). The cohesive law may be written on the form: $\tau = f(\delta, \tau_0, \delta_c)$ where τ_0 is the onset traction and δ_c is the critical separation at which complete separation occurs and new traction-free crack faces ($\tau = 0$) are formed. When the crack opening displacement equals the critical separation ($\delta = \delta_c$) at the trail of the cohesive zone, as illustrated in Fig. 1.7(a), the crack is said to be critically loaded. The function f controls the shape of the cohesive law, which highly depends on the damage mechanisms operating in the FPZ. Generally, under small-scale FPZ conditions, the shape of the cohesive law is insignificant (Alfano, 2006). However, under certain conditions, and particularly when large-scale fibre bridging prevails, the shape of the cohesive law becomes important and advanced cohesive laws are necessary. Advanced cohesive laws are discussed further in later sections (Sec. 2.1.2).

The work of separation, Γ_c, per unit area of crack face is defined by $\Gamma_c = \int_0^{\delta_c} \tau(\delta) d\delta$ (units: J/m^2), which is often used besides the cohesive parameters: τ_0 and δ_c. By use of the path-independent J-integral (Rice, 1968) it can be shown that the work of separation per unit crack area of a critically loaded crack equals the critical ERR: $\Gamma_c = G_c$. Accordingly, at complete separation the energy released (i.e. dissipated energy) per unit crack area equals the material property G_c.

The energy dissipation during crack growth is a continuous and irreversible process for each point in the cohesive zone. An illustrative example showing the irreversible damage process during a loading-unloading sequence of a material point in the cohesive zone is illustrated in Fig. 1.8(a)-1.8(d) (Bak, 2015, 2017). Further details on constitutive damage modelling in a CZM formulation is provided in paper A. Irreversible damage develops when the crack opening displacement related to the onset traction, τ_0, is reached. As the load increases monotonically, the separation process causes a reduced cohesive traction according to the softening cohesive law, see Fig. 1.8(b). Upon unloading the crack, i.e. closing the crack faces, the (δ, τ)-relation typically decreases linearly towards $(0;0)$ as shown in Fig. 1.8(c). In order to ensure irreversibility, a damage parameter $d = \Gamma_d/\Gamma_c$ (or similar) is introduced, which updates the shape of the cohesive law as the separation process progresses. An updated cohesive law following the loading-unloading sequence is shown in Fig. 1.8(d). Notice the division of areas under the (δ, τ)-relation into dissipated specific energy, Γ_d, and the remaining specific energy, i.e. the remaining ability to perform specific work ($\Gamma_c - \Gamma_d$).

Experimental characterisation of the cohesive law is discussed Sec. 2.1.3.
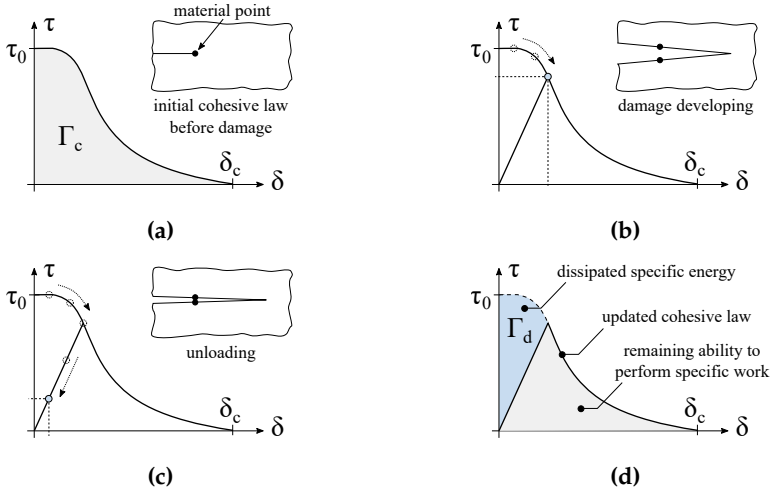
Fig. 1.8: Schematic outline of irreversible crack growth during a loading-unloading sequence. The figure is copied from (Bak, 2015, 2017) with minor modifications.

Mixed-mode cohesive laws

Delaminations in laminated FRP composite materials often propagate under mixed-mode conditions, as explained in Sec. 1.2.1, which must be taken into account in the CZM. To develop a mixed-mode cohesive law, three basic considerations are required: *I)* A mode-dependent initiation criterion, *II)* a mode-dependent propagation criterion, and *III)* criteria to ensure irreversible damage under variable crack opening mode and loading-unloading sequences.

   Damage initiates when the traction equals the onset traction, τ_0, and propagation occurs when the work of separation, Γ, equals the critical ERR, G_c. For pure mode I crack opening the criteria becomes:

$$\tau = \tau_I^0 \text{ (Initiation)} \tag{1.2}$$

$$\Gamma = G_{Ic} \text{ (Propagation)} \tag{1.3}$$

similar relations can be written for pure mode II and pure mode III cracking. In mixed-mode cracking problems, mode interaction effects must be taken into consideration in the initiation and propagation criteria. Several mixed-mode crack initiation and propagation criteria are available in the literature. For example, damage initiation criteria are often based on the delamination onset criterion proposed in (Ye, 1988) for graphite/epoxy laminates:

$$\left(\frac{\langle \tau_3 \rangle}{\tau_I^0} \right)^2 + \left(\frac{\tau_2}{\tau_{II}^0} \right)^2 + \left(\frac{\tau_1}{\tau_{III}^0} \right)^2 = 1 \tag{1.4}$$

where τ_3 is the traction component normal to the crack plane, and τ_1 and τ_2 are the in-plane shear traction components in the basic directions. Notice that the criterion in Eq. (1.4) provides quadratic interaction of the traction components. The delamination propagation criterion is usually a mode interaction criterion established in terms of the mode-decomposed ERRs ($G_I, G_S = G_{II} + G_{III}$) and the corresponding critical ERRs ($G_{Ic}, G_{IIc}(= G_{IIIc})$). For example the Benzeggagh-Kenane (BK) mode interaction criterion to predict mixed-mode delamination propagation in UD glass/epoxy composites (Benzeggagh and Kenane, 1996):

$$G_c = G_{Ic} + (G_{IIc} - G_{Ic}) \left(\frac{G_S}{G_T} \right)^{\eta} \tag{1.5}$$

where $G_T = G_I + G_{II} + G_{III}$ and delamination propagation occurs if $G_T \geq G_c$ in Eq. 1.5.

Finally, the mixed-mode cohesive law must possess a criterion to ensure irreversible crack growth under varying crack opening mode. This is controlled by damage models that convert the damage state if the crack opening mode is changed from one degree of mode-mixity to another. A mixed-mode constitutive damage model is derived in paper A for an advanced cohesive law. The reader is referred to paper A in appendix for further details.

In mixed-mode cracking problems, the degree of mode-mixity is commonly established in terms of a mode-mixity ratio, which have different definitions depending on the application and theoretical framework. For experimental characterisation of fracture properties, the degree of mode-mixity is commonly defined as a ratio of mode decomposed ERRs, which provides a global mode-mixity ratio (and may be evaluated using the mode-decomposed J-integral approach (Huber et al., 1993; Rigby and Aliabadi, 1998; Carreras et al., 2019)).

In CZM formulations, the mode-mixity ratio is evaluated locally at every material point (i.e. integration point in a FE formulation) in the cohesive zone. Different CZM formulations possess different definitions. For example, the local mode-mixity ratio is defined as the ratio of the accumulated mode II and total dissipated energy at a given integration point in (Camanho et al., 2003) such that the mixed-mode ratio depends on the load history. Another local mode-mixity ratio is applied in the CZM formulated in (Turon et al., 2006), which defines an instantaneous mode-mixity ratio as the ratio of the current normal and tangential nodal displacement components. Generally, under mixed-mode crack growth the local mode-mixity ratio varies throughout the cohesive zone even if the global mode-mixity, e.g. based on the mode-decomposed J-integral, remains constant (Turon et al., 2010; Sarrado et al., 2012).

1.5 Fatigue-driven delamination

1.5.1 Fatigue crack growth

Fatigue-driven delamination is sub-critical crack growth under cyclic loading. Experimental observations show that the crack growth rate, da/dN (where a and N denotes the crack length and number of load cycles, respectively), follows a linear trend when plotted against the cyclic SIF range, ΔK, on a log-log scale. The relation is known as Paris' law (Paris et al., 1961; Paris and Erdogan, 1963), which is currently the most common applied approach to fatigue crack growth:

$$\frac{da}{dN} = C\Delta K^n \tag{1.6}$$

where C and n are curve fitting parameters. The power law-relation in Eq. (1.6) is an empirical correlation that originated from successful studies on metal fatigue, and it has subsequently been adopted to assess fatigue-driven delamination in laminated FRP composite materials. A common practice, however, is to replace the SIF, K, by the ERR, G, in Paris' law, as illustrated in Fig. 1.9(a). The practice is primarily due to the difficulty of computing the near crack tip stress field (SIF) in laminated inhomogeneous materials (Rans et al., 2011). The cyclic ERR range, ΔG, and the maximum value of the cyclic ERR, G_{max}, are the most commonly used parameters in experimental characterisation of fatigue-driven delamination. The direct equivalence of ΔK, cf. Eq. (1.6), is actually $(\Delta\sqrt{G})^2$, which has also been applied for characterisation of fatigue-driven delamination growth, e.g. (Rans et al., 2011).

The distinction between the ERR, G, and the SIF, K, in Eq. (1.6) may not be critical since the Paris law is an empirical correlation (Pagano and Schoeppner, 2000). The independent variable may be arbitrarily chosen among the different formulations of G (e.g. G_{max} and $(\Delta\sqrt{G})^2$) with respect to fitting the crack growth rate data in a Paris law-like relation. Depending on the scope of the analysis, other opinions on this matter are expressed in literature as well, e.g. (Rans et al., 2011).

So far no standardised procedure for characterisation of fatigue-driven delamination growth in laminated FRP composite materials has been established. Nevertheless, standardised test methods exist for characterisation of the mode I interlaminar fracture toughness (ASTM D5528) and the mode I fatigue delamination growth onset (ASTM D6115) of uni-directional laminated FRP composite materials. These test methods utilise the double cantilever beam (DCB) specimen subjected to opening point loads at one end of the DCB specimen as illustrated in Fig. 1.9(b). The same DCB test configuration
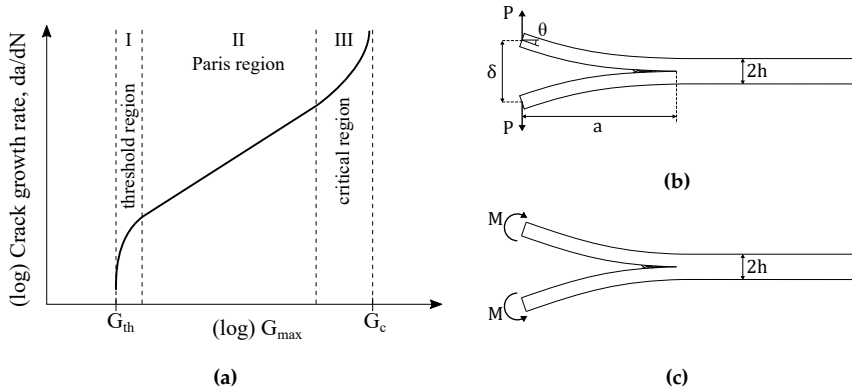
Fig. 1.9: (a) Paris law-like relation in terms of the maximum ERR, G_{max}. (b) Conventional mode I DCB test, where P is the opening force, δ is the crack mouth opening displacement, a is the crack length, B is the specimen width, and θ is the rotation of the DCB arm load introduction. (c) The pure moment loaded DCB specimen. Notice that the DCB arms in Fig. (b) and (c) deform differently: The curvature in (c) is constant.

is widely applied in the literature to obtain mode I ($G_{max}, da/dN$)-curves (or similar) of laminated FRP composite materials. The test specimen configuration in Fig. 1.9(b) will be referred to as the conventional DCB test in the following due to its wide application for characterisation of mode I fatigue-driven delamination.

A fatigue test using the conventional DCB test configuration is usually conducted in displacement- (δ) or load-control (P). The ERR of the conventional DCB test can be computed by the J-integral, $G = J = 2P\theta/B$ (Anthony and Paris, 1988; Suo et al., 1992; Sørensen and Jacobsen, 2000), which can be rewritten using simple beam theory such that $G = 3P\delta/2Ba$. Various corrections are proposed in the literature to improve the accuracy of this calculation, e.g. shear correction and the effect of DCB arm root rotation (Hashemi et al., 1989, 1990a). The ERR of the conventional DCB test depends on the crack length, a, thus the ERR may gradually decrease or increase as the crack propagates depending on the control-mode. Consequently, the conventional DCB test is able to sweep a wide range of ERR values and crack growth rates during a single test under constant amplitude displacement- or load-control, which in principle enables one to measure a complete Paris' law.

Finally, two complications of the conventional DCB test configuration are highlighted, which will be revisited in later sections and in paper D. Firstly, when a large-scale fibre bridging exists, the ERR depends on the crack length and distribution of tractions in the FPZ (Suo et al., 1992; Sørensen and Jacobsen, 2000). Secondly, the conventional DCB test configuration is not a steady-state specimen. A steady-state specimen means that once the fibre bridging

zone is fully developed, the crack growth can occur in a steady-state fashion, in the sense that the fibre bridging zone maintains its size and translates along with the crack tip in a self-similar manner (Suo et al., 1992; Sørensen and Jacobsen, 2000; Sørensen, 2016). The pure moment loaded DCB specimen, which is illustrated in Fig. 1.9(c), is a steady-state specimen, and will be considered in later sections.

1.5.2 Real load spectra

The fatigue loads acting on a structure in-service are generally referred to as the in-service load spectrum or the real load spectrum. To highlight characteristics of real load spectra, an example is provided in Fig. 1.10, which illustrates the root bending moment-time history of a wing on a transport aircraft. The example is based on an example provided in (Schijve, 2009).

During flight, the distributed aerodynamic lift on the wing carries the weight of the aircraft and causes a bending moment on the wing with maximum value at the root of the wing. The bending moment introduces tensile stresses at the lower wing skin structure and compressive stresses at the upper wing skin structure. On ground the aerodynamic lift is zero and the weight of the aircraft is carried by the undercarriage. Thus each flight involves one cycle (ground-air-ground) of the bending moment as indicted by the thick solid line in Fig. 1.10, which is a very slow load cycle (almost quasi-static variation of the load). The wing is also subjected to loads of higher frequency. In the "air"-period, cf. Fig. 1.10, high frequency loading occurs due to turbulence (gusty weather) primarily during the climb- and descent-phases at relatively low altitudes. The turbulence during cruising at high altitudes is usually low and neglected in Fig. 1.10. Notice also the linearly decreasing load during cruise, which is explained by the aircraft's reduced weight due to fuel consumption. Manoeuvre loads (e.g. dynamic, gravitation, etc.) can also be significant (especially in a fighter aircraft). During take-off and landing, high-frequency load cycles are introduced due to runway roughness, touch down, and other matters.

The example illustrates two characteristic features of real load spectra: Generally, a real load spectrum is a complex mix of I) deterministic loads and II) stochastic loads (Farrow, 1996). A load is considered to be deterministic if the magnitude of the load event can be estimated and the instant at which it occurs in the load-time history is predictable. Deterministic loads can often be determined from the expected utilization of a structure, e.g. load cycles due to the aerodynamic lift on the aircraft wing, and manoeuvre loads. Stochastic loads (also referred to as random loads) cannot be predicted to occur with a certain magnitude at a given time instant; a description is possible only with the application of statistics and probability calculus (Schijve, 2009; Köhler et al., 2017). In the aircraft example, stochastic loads are exemplified
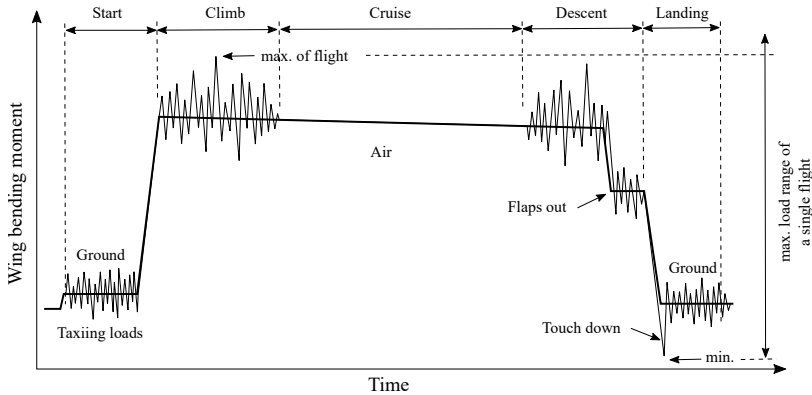
Fig. 1.10: Schematic outline of the load-time history of the wing of a transport aircracft. Bending moment at the wing root. The figure is reconstructed from Fig. 9.5 in (Schijve, 2009).

by the effect of turbulence and runway roughness. Stochastic and deterministic loads may occur simultaneously which may give rise to load peaks, e.g. the max. bending moment in Fig. 1.10.

Standardized load spectra have been developed based on samples of recorded load-time histories to account for the in-service loads in various practical applications. An overview is provided in (Heuler and Klätschke, 2005). Examples of standardized load spectra are: The TWIST load spectrum representing the wing root bending moment of a transport aircraft (Schütz et al., 1973), the FALSTAFF load spectrum representing the load-time histories (manoeuvre dominated) at the wing root of fighter aircraft (Aicher et al., 1976), the WISPERX load spectrum representing the flapwise bending of horizontal axis wind turbine blades (ten Have, 1992), and the CARLOS load spectrum representing load-time histories of front wheel suspension parts in cars (Schütz et al., 1990).

1.5.3 Load interaction effects

The real load spectra acting on structures in service are certainly complex variable amplitude (VA) load spectra. The VA load spectra are significantly different from the constant amplitude (CA) sinusoidal waveforms applied to test specimens for characterisation of fatigue properties, e.g. the Paris' law. The most common approach to assess the fatigue damage accumulation in composites subjected to VA loading is by using linear damage accumulation rules, e.g. the Palmgren-Miner damage accumulation law (Palmgren, 1924; Miner, 1945). A simple (and the most logical) approach to compute the fatigue crack growth under VA loading is exemplified in Eq. (1.7). The growth of a pre-existing crack of initial length a_0 under VA loading can be predicted

by direct summation of crack increments in a cycle-by-cycle approach. The crack length, a_N, after N load cycles becomes:

$$a_N = a_0 + \sum_{i=0}^{N} \Delta a_i = a_0 + \sum_{i=0}^{N} f(G_{max,i}, R) \tag{1.7}$$

where the crack growth increment, Δa_i, associated with a given load cycle, i, of VA loading can be estimated from the $(G_{max}, da/dN)$-curve (or similar) obtained under CA loading at a given load ratio, R, e.g. Fig. 1.9(a). The direct summation approach accounts for every load cycle in the load spectrum; it assumes that the crack growth increment related to each load cycle is not influenced by prior load cycles. A similar practice is exercised in the majority of state-of-the-art delamination prediction models, e.g. fatigue CZM (Bak et al., 2014), which commonly evaluate the current damage growth increment based on the instantaneous cyclic variation of mode-decomposed energy release rates, however, neglect any influence of the load history. These approaches are also known as non-interaction models.

A fundamental shortcoming of non-interaction models is the neglection of the load history. The term load interaction effect is commonly used to label the phenomenon that the crack growth increment in a given load cycle depends on the damage caused by preceding load cycles. Load interaction effects may accelerate or retard the crack growth under VA loading, leading to possible non-conservative life-predictions. However, little research is conducted in this field, which will be considered further in the literature review in Sec. 2.2.

1.6 Objectives of the PhD project

The project investigates delamination in laminated FRP composite materials with complex FPZ due to fibre bridging under quasi-static loading and VA fatigue loading. In overall terms, the scientific work may be divided into two tasks: I) Develop computational methods to simulate delamination growth under quasi-static loading when large-scale fibre bridging prevails. II) Set up and run experimental test campaigns to understand and characterise the progression of delamination growth and governing mechanisms under VA loading.

Part I takes point of departure in the CZM framework. To simulate delamination with fibre bridging it is necessary to implement advanced cohesive laws in the CZM formulation, which requires developing new constitutive damage models, and to develop characterisation methods to obtain model parameters of the advanced cohesive laws. Part II is concerned with a research area of very little research with many unsolved problems (see Sec.
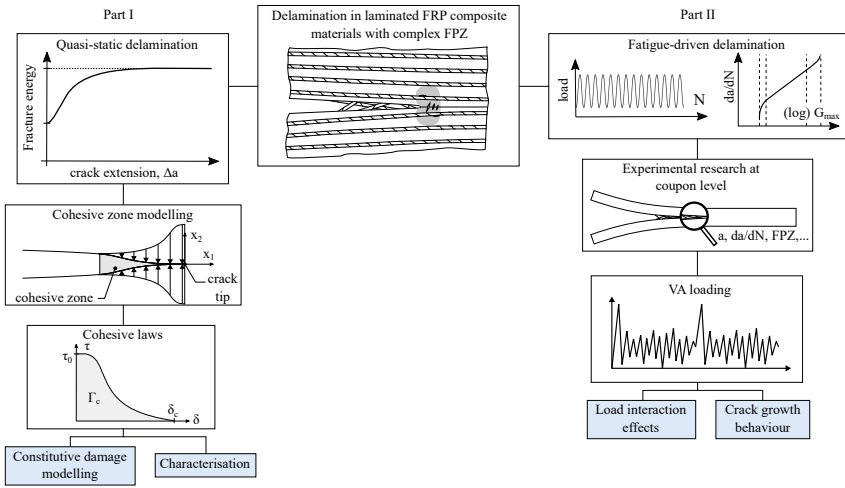
Fig. 1.11: Schematic outline of research topics in hierarchical structure. The blue rectangles indicate the research topic under consideration in the following sections and papers A-D.

2.2). The long term aim of part II is to be able to develop delamination prediction models capable of considering load interaction effects to accurately simulate delamination under VA loading. However, experimental research is a necessary precursor to understand fatigue-driven delamination and governing mechanisms (e.g. fibre bridging) under VA loading. Therefore, Part II conducts experimental test campaigns to characterise fatigue-driven delamination under VA loading with emphasis on load interaction effects. The test campaign must quantitatively measure the progression of the actual delamination growth behaviour under VA loading. An undesirable alternative is stand-alone measurements of the fatigue life and/or the degradation of macroscopic specimen properties.

An overview of part I and part II and the associated research topics is provided in Fig. 1.11 in a hierarchical structure. The objectives of the work are summarised in the items listed below:

I) Develop a CZM with an advanced cohesive law formulation capable of accounting for complex FPZ - specifically large-scale fibre bridging.

II) Develop a robust and efficient methodology for characterisation of advanced cohesive laws.

III) Develop and conduct experimental campaigns to understand and characterise delamination growth and governing mechanisms under VA loading. Special attention should be given to load interaction effects.

Item no. *I)* is the topic in paper A. Item no. *II)* is considered in paper B. Item no. *III)* is investigated in papers C-D.

2

State-of-the-Art Literature Review

The introductory chapter has introduced basic concepts and the necessary background to the topics dealt with in this thesis. In this chapter, a literature review of state-of-the-art in the research fields of interest is provided. Firstly, attention is given to advanced cohesive laws in the quasi-static CZM framework, which is related to papers A and B. Secondly, the literature review focuses on fatigue in laminated FRP composite materials under VA loading with special emphasis on fatigue-driven delamination. Experimental works are primarily considered in the second part, which is related to papers C and D.

2.1   Cohesive zone models with R-curve behaviour

2.1.1   Basic FEM implementations

Practical application of the CZM involves implementation in a FEM framework. Several FE implementations of the CZM is applied in academia and in the industry to simulate delamination (Bak et al., 2014; Park and Paulino, 2011; Tabiei and Zhang, 2018). The intention of the current section is to provide a brief overview of different FE implementations of the CZM, and to pinpoint the formulation selected for the work in papers A-B.

The CZM formulation can be implemented in FEM frameworks following two main procedures according to (Moës and Belytschko, 2002): Discrete intra-element cracks and discrete inter-element cracks. The intra-element approach allows a displacement jump (i.e. strong discontinuity) inside a finite element, where a cohesive law can be used to control the separation process (energy dissipation). The displacement jump can be embedded inside the element in several ways, e.g. by use of the extended finite element method (XFEM) where the crack can be represented with discontinuous shape func-

tions (Moës et al., 1999), or by remeshing of sub-domains using the floating node method (FNM) (Chen et al., 2016). In the inter-element crack approaches the crack extends between elements. A cohesive zone can be represented as an interface element in between each pair of neighbouring elements in the mesh (Xu and Needleman, 1994; Camacho and Ortiz, 1996). The interface element is the most common implementation of the CZM for analysis of cohesive crack growth in laminated composite materials and the most matured method in commercial FEM codes.

There are two overall formulations of the interface element available in the literature. The interface element may be implemented within a potential crack path prior to computational simulation, which is known as an intrinsic CZM. Alternatively, the interface elements can be inserted adaptively during computational simulation whenever a certain criterion is met and wherever needed. The latter approach is know as an extrinsic CZM (Park and Paulino, 2011). The extrinsic approach requires sophisticated algorithms to insert interface elements which is challenging for 3D models and parallel computing. The intrinsic interface elements require an initial elastic constitutive relationship prior to damage onset (as illustrated in Fig. 2.1(b) for $0 \geq \lambda \geq \lambda_0$). The initial elastic behaviour possess a finite stiffness, also known as the penalty stiffness, K, which introduces artificial compliance to the model. The artificial compliance may become an issue when interface elements are implemented between every element interface, but usually negligible when only several layers of interface elements are implemented, such as a delamination problem (Tabiei and Zhang, 2018). The intrinsic interface element approach requires one to define the potential crack path a priori, which is usually possible in laminated composite materials since cracks are prone to grow along layer interfaces. The intrinsic interface element formulation is the selected framework for the CZM developed in the present work (papers A-B).

Intrinsic interface element in an equivalent one-dimensional formulation

A schematic outline of basic mechanical concepts of an intrinsic interface element is shown in Fig. 2.1. The interface element introduced here is based on the widely used quasi-static damage model in (Turon et al., 2006) which can be considered as an extension of the CZM in (Camanho et al., 2003).

In the undeformed configuration a potential crack path is modelled as a surface S^0 through the continuum body. The surface allows for a displacement (strong) discontinuity across the interface, which is described by an upper and lower crack face S^+ and S^-, respectively. In the deformed configuration, the kinematic model is described according to a mid-surface, $\bar{S}$, which is defined as the average distance between initially coincident points in the upper, S^+, and lower, S^-, surfaces. The interface separation in the global Cartesian coordinate system is described by $(u^+ - u^-)$. The local separation
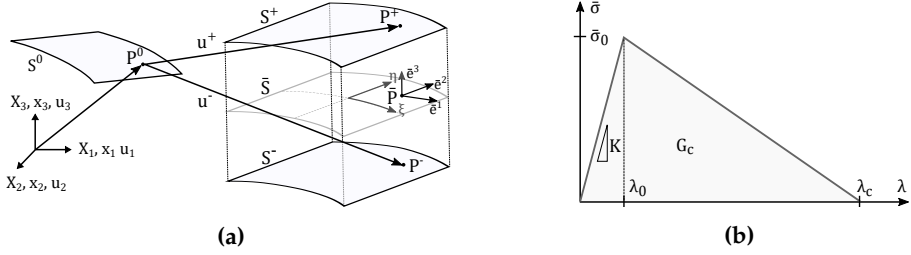
Fig. 2.1: Basic mechanics of an intrinsic interface element for CZM (a) Kinematic model. (b) Bilinear cohesive law shown for a given degree of mode-mixity.

vector, $\mathbf{\Delta}$, can be computed using a transformation tensor, $\mathbf{\Theta}$, which can be derived from a local coordinate system (ξ, η) defined at the mid-surface, $\bar{S}$, such that $\mathbf{\Delta} = \mathbf{\Theta}(\mathbf{u}^+ - \mathbf{u}^-)$. An interface constitutive law relates interface separations, $\mathbf{\Delta}$, to cohesive tractions, $\boldsymbol{\tau}$:

$$\tau_i = (1-d)D^0_{ij}\Delta_j - dD^0_{ij}\delta_{3j}\langle -\Delta_3 \rangle \tag{2.1}$$

where $D^0_{ij} = K\delta_{ij}$, and the Macaulay bracket, $\langle x \rangle = \frac{1}{2}(x + |x|)$, in the second term ensures that the stiffness equals to the penalty stiffness in case of negative normal opening, $\Delta_3 < 0$. The scalar damage parameter, d, degrades the cohesive interface stiffness. The evolution of d is controlled by a damage model and a mixed-mode bilinear cohesive law in an equivalent one-dimensional formulation as illustrated in Fig. 2.1(b). The equivalent one-dimensional formulation relates the interface separation norm, λ, and the equivalent one-dimensional cohesive traction, $\bar{\sigma}$, as defined here:

$$\bar{\sigma} = K(1-d)\lambda \qquad \lambda = \sqrt{\Delta_s^2 + \langle \Delta_3 \rangle^2} \quad \text{for} \quad \Delta_s = \sqrt{\Delta_1^2 + \Delta_2^2} \tag{2.2}$$

The equivalent one-dimensional formulation possesses an opening path dependence, in contrast to another common formulation of mixed-mode cohesive laws, e.g. the potential-based CZM. A comparison of these formulations can be found in (Park and Paulino, 2011). In paper A, a mixed-mode cohesive law is derived in an equivalent one-dimensional formulation for an intrinsic interface element. The work takes point of departure in the framework in (Turon et al., 2006) and a similar bilinear mixed-mode cohesive law, which has been implemented in a user-programmed interface element for ANSYS Mechanical in (Lindgaard et al., 2017). The reader is referred to paper A for further details on the CZM interface element formulation.

2.1.2 Advanced cohesive laws

One of the main attractive features of the CZM is its convenience and simplicity in simulation of complex cracking processes. This is basically accomplished by smearing together all the underlying damage mechanisms in a traction-separation relation, which controls the energy dissipation during the cracking process. The traction-separation relation becomes very important in this regard, as it should reflect the underlying damage mechanisms in the FPZ. The CZMs in the previous section (Camanho et al., 2003; Turon et al., 2006; Lindgaard et al., 2017) utilise a bilinear cohesive law as illustrated in Fig. 2.1(b), which has also been widely applied by others, e.g. (Mi et al., 1998; Chen et al., 1999; Alfano and Crisfield, 2001; Segurado and Llorca, 2004). The bilinear cohesive law is one of the simplest representations of the softening response after damage onset. It is pragmatic as the shape is completely defined by two independent cohesive parameters[1], e.g. the onset traction, τ^0, and the fracture toughness, G_c, (the critical separation becomes $\delta_c = 2G_c/\tau^0$). However, the bilinear cohesive law provides little information on the separation process. In addition to the bilinear cohesive law there are other commonly applied shapes, such as rectangular (Dugdale, 1960), trapezoidal (Tvergaard and Hutchinson, 1992), exponential (Ortiz and Pandolfi, 1999; Goyal et al., 2004), and linear-parabolic shapes (Allix et al., 1995).

An investigation on the influence of the shape of cohesive laws in numerical simulation of pure mode delamination under small-scale FPZ conditions is performed in (Alfano, 2006). The study compares four different shapes: Bilinear, trapezoidal, exponential, linear-parabolic, while keeping the onset traction, τ^0, fracture toughness, G_c, and penalty stiffness, K, fixed. It is found that the importance of the shape of the cohesive law depends on the boundary value problem; in a typical DCB test the simulated load-displacement curve is observed to be practically independent of the shape. For other problems, the shape of the cohesive law only has an influence in the vicinity of the maximum applied load. In terms of the algorithmic numerical performance (numerical stability, convergence), a difference is observed. The bilinear shape is concluded to be the best compromise between computational cost and the degree of approximation achieved (Alfano, 2006).

The study by (Alfano, 2006) is aligned with the general assumption that the shape of the cohesive law is insignificant in the prediction of fracture under small-scale FPZ conditions. However, when large-scale FPZ conditions prevail, the shape of the cohesive law becomes important (Bao and Suo, 1992; Sørensen and Jacobsen, 1998). In the FPZ of a delamination crack, see Fig. 1.3, several damage mechanisms co-exist and operate at different length

---

[1]In addition, the penalty stiffness, K, must be defined, however, this is more or less a numerical tuned parameter
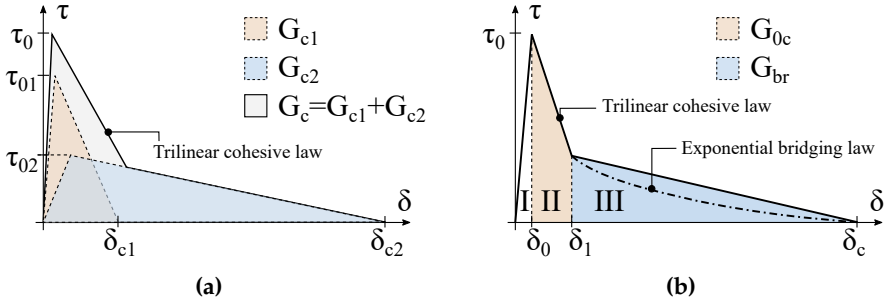
Fig. 2.2: (a) Obtaining a trilinear cohesive law by superposition of two bilinear cohesive laws following the approach in (Dávila et al., 2009). (b) Trilinear cohesive law in three-part following the approach in (Tamuzs et al., 2001). The exponential bridging law in part III corresponds to the approach in (Sorensen et al., 2008).

scales. Typically, fibre bridging operates at large crack opening displacements ($\delta \approx 1 - 10$ mm) with relatively low cohesive tractions ($\tau \approx 1$ MPa). Thus, the bridging mechanism introduces a characteristic tail on the cohesive law as illustrated in Fig. 2.2. Notice that a relatively large fracture energy (i.e. the area under the traction-separation relation at the tail) is associated with the fibre bridging mechanism.

The cohesive laws treated previously are commonly referred to as *simple* cohesive laws (Dávila et al., 2009) due to their simple shape and the few necessary cohesive parameters to completely define the traction-separation law (e.g. τ^0, G_c (and K)). The simple cohesive laws are inadequate to take the complex softening response of several co-existing damage mechanisms into account. Alternatively, *advanced* cohesive laws can be applied, which typically involves complex shaped traction-separation relations and requires additional cohesive parameters, such as parameters defining the transition from one cohesive relation to another (examples follow).

A procedure to represent multiple damage mechanisms in the FPZ considering fibre bridging is proposed in (Dávila et al., 2009; Airoldi and Dávila, 2012). The procedure superposes two bilinear cohesive laws each representing a distinct damage mechanism (Dávila et al., 2009): One bilinear cohesive law is associated with quasi-brittle fracture at the crack tip, which is characterised by a short critical separation, δ_{c1}, and a high onset traction, τ_1^0, as illustrated in Fig. 2.2(a). Another bilinear cohesive law is associated with fibre bridging, which is characterised by a lower onset traction, τ_2^0, and a large critical separation, δ_{c2}. The resulting cohesive law possesses a bilinear softening response, i.e. the cohesive law is said to be trilinear. The trilinear cohesive law has been successfully applied in other previous works to investigate R-curve behaviour in delamination with fibre bridging (Tamuzs et al.,

2001; Heidari-Rarani et al., 2013; Airoldi and Dávila, 2012). For example, the three-part division of the cohesive law in (Tamuzs et al., 2001) as illustrated in Fig. 2.2(b), where G_{c0} is the specific fracture energy associated with crack tip quasi-brittle fracture, and G_{br} is the specific fracture energy associated with large-scale fibre bridging. A similar approach is applied to model mode I delamination with fibre bridging in (Sorensen et al., 2008), where the third part of the cohesive law in Fig. 2.2(b) is replaced by a an exponential decaying bridging law as shown in the figure.

The trilinear cohesive law assumes a simple linear variation of bridging tractions over a relatively large range of crack opening displacement (see $\delta_1 \leq \delta \leq \delta_c$ in Fig. 2.2(b)). Although this is pragmatic, it is often inaccurate with respect to the actual variation of bridging tractions. For example, the micromechanical model of cross-over fibre bridging in (Sørensen et al., 2008) derives a relation on the form $\tau \propto 1/\sqrt{\delta}$ for mode I crack opening, see Sec. 1.3.2. Additionally, in order to utilise the tri-linear cohesive law (Tamuzs et al., 2001; Dávila et al., 2009; Heidari-Rarani et al., 2013; Airoldi and Dávila, 2012), or the linear-exponential softening law (Sorensen et al., 2008), a high degree of expertise concerning the material system and governing damage mechanisms is necessary to impose a priori shape assumptions.

The cohesive law can be less restrictive in shape, such that very few/no a priori shape assumptions are required. An arbitrary shaped cohesive law can be accomplished by a spline (e.g. linear or cubic) representation. The spline-representation is versatile and can be adapted to arbitrary damage mechanisms in the FPZ. A linear and cubic Hermite spline-based cohesive law for mode I CZM is developed in (Shen et al., 2010) and applied in (Shen and Paulino, 2011) to investigate fracture in adhesively bonded PMMA specimens and Garolite (woven glass cloth in an epoxy resin) specimens. A similar cubic spline-based cohesive law is applied in (Xu et al., 2017) to simulate adhesive failure. A mixed-mode capable linear spline-based cohesive law has recently been successfully applied in CZM of a different material system in (Pereira et al., 2017, 2018). Mode I and mode II fracture in bovine cortical bone is investigated using a piecewise linear (four line segments) cohesive law implemented in an ABAQUS user-element subroutine (Pereira et al., 2017, 2018).

Finally, environmental effects on interface constitutive properties is often a research topic of interest, see e.g. (Katnam et al., 2010; Abdel-Monsef et al., 2019, 2020; Pereira et al., 2012). The spline-based cohesive laws are highly versatile and possess a high degree of freedom, which is valuable in this regard, for example to determine the effect of moisture on the material softening law. The spline-based cohesive laws possess interesting and unexploited properties with respect to delamination analysis in FRP composite materials with large-scale fibre bridging. For this purpose, a linear spline-based mixed-mode cohesive law is developed in paper A. It is noticed, that the work in paper A

is simultaneous and independent of the work in (Pereira et al., 2017, 2018), which has a different formulation with respect to paper A and has been applied to a completely different material system.

2.1.3 Characterisation of cohesive laws

When the shape of the cohesive law is insignificant, e.g. under small-scale FPZ conditions, the necessary cohesive parameters (G_c, τ^0) can be derived from more or less standardised test procedures. For example, the fracture toughness under mode I and mixed mode I/II fracture can be determined from the DCB test (ASTM D5528) and the mixed-mode bending (MMB) test (ASTM D6671), respectively, whereas the mode II fracture toughness is typically determined using the end notched flexure (ENF) test. The onset tractions are typically determined as a certain fraction of the laminate's out-of-plane strength for which standard testing procedures also exist. However, when the shape of the cohesive law is important, there are no standard characterisation procedures available.

Many approaches have been proposed to obtain the traction-separation relation. The approaches may be classified as direct or inverse/iterative methods (Gowrishankar et al., 2012). The direct methods extract the cohesive law without recourse to extensive numerical analysis. The inverse methods, by contrast, determine the cohesive law by iteratively comparing solutions obtained from parametric numerical models and experimental measurements.

Experimentally, the stable uni-axial tensile test may be considered the most fundamental method to directly determine the traction-separation relation (Petersson, 1981). In the direct uni-axial tensile test a specimen is subjected to uni-axial tension, and the damage evolution across the specimen width must be uniform in the gauge section. An extensometer measures the relative displacement between two points across the failure plane, then subtracting the elastic deformation of the gauge section provides the opening of the cohesive law. However, the uni-axial tensile test is difficult to realise for several issues related to multiple cracking, pre-cracking, asymmetric failure modes and non-uniform crack opening across the specimen. For a complete description of difficulties related to the uni-axial tensile test to measure traction-separation relations, the reader is referred to (Elices et al., 2002; Petersson, 1981; Sørensen and Jacobsen, 2000).

Another direct method extracts the traction-separation relation based on measurements of the crack opening profile in the vicinity of the FPZ (Cox and Marshall, 1991). A popular direct method is to derive the cohesive law from measurements of the J-integral and the end-opening displacement of the cohesive zone (Li and Ward, 1989; Sørensen, 2016). The J-integral approach is briefly summarised here and illustrated in Fig. 2.3. The path-independent
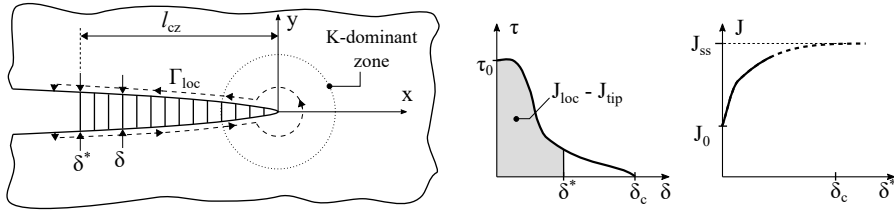
Fig. 2.3: Large-scale FPZ in comparison to the K-dominant zone. Bridging tractions exist in the crack wake due to the presence of fibre bridging.

J-integral can be evaluated locally along an integration path Γ_{loc} according to Eq. (2.3). The integration path, Γ_{loc}, follows the crack faces and encloses the cohesive zone and the crack tip as shown in Fig. 2.3. The end-opening displacement of the cohesive zone are denoted by δ^* and the quantity J_{tip} represents the J-integral evaluated around the crack tip. During loading of a specimen having a sharp pre-crack (i.e. initially unbridged crack faces), crack growth is assumed to occur when J_{tip} equals the critical fracture energy of the crack tip, J_0 (Sørensen, 2016). As the crack tip extends, a fibre bridging zone develops between the initial crack tip and the current crack tip position. The cohesive zone length, l_{cz}, and the end-opening displacement, δ^*, increases as the crack extends, which increases the fracture resistance in accordance with Eq. (2.3). When the end-opening displacement reaches the critical separation, $\delta^* = \delta_c$, the fracture resistance attains a maximum value, J_{ss}. By definition J_R is the value of the J-integral during crack growth. Differentiation of J_R with respect to the end-opening displacement, δ^*, gives the cohesive traction (Suo et al., 1992; Li and Ward, 1989), see Eq. (2.4).

$$J_{loc} = \int_0^{\delta^*} \tau(\delta)d\delta + J_{tip} \tag{2.3}$$

$$\tau(\delta^*) = \frac{\partial J_R}{\partial \delta^*} \tag{2.4}$$

The J-integral technique is well-suited for the pure moment loaded DCB specimen for which a simple closed-form solution of the J-integral can be determined - even for large-scale FPZ conditions. The J-integral approach is applied to delamination problems in FRP laminates with large-scale fibre bridging in (Sørensen and Jacobsen, 2003; Sørensen and Kirkegaard, 2006).

The inverse methods iteratively adjust certain model parameters in order to minimise an error function, which describes the discrepancy between responses obtained from parametric numerical models and experiments. Generally, the inverse methods are computationally expensive and inverse problems are likely to be ill-posed. Therefore, the inverse methods should be ef-

ficient, i.e. converge to an optimal solution within few iterations, and robust, i.e. converge to the same optimal solution for different initial guesses, etc. Common characteristics of inverse methods are summarized in (Elices et al., 2002). The inverse methods typically rely on global structural responses, e.g. load versus crack mouth opening displacement (CMOD), from popular notched beams or compact specimens (Elices et al., 2002). For example, in (Bouhala et al., 2015) an error function is defined in terms of load-displacement curves from a DCB experiment and parametric finite element model (XFEM CZM formulation) to identify the model parameters of a mode I bilinear cohesive law of CFRP laminates.

The error functions in inverse methods may also be defined from local kinematic measurements in the vicinity of the crack tip, e.g. local crack opening displacements and full-field digital image correlation (DIC) measurements of the displacement-field (Shen et al., 2010; Shen and Paulino, 2011; Alfano et al., 2015).

The inverse methods often search directly for model parameters in a CZM framework such that the inverse method directly outputs a traction-separation relation. However, the inverse parameter identification may also be based on a parametric FE model without CZM, which is the approach followed in (Sorensen et al., 2007). An inverse methodology is proposed in (Sorensen et al., 2007) for identification of bridging tractions in UD carbon fibre reinforced polymer (CFRP) composites under mode I delamination using distributed local strain measurements from fibre Bragg grating (FBG) sensors, which have been embedded parallel to the reinforcing fibres during consolidation. The FBG sensors measure the internal axial strain distribution above the delamination plane over several millimetres along the delamination direction. A 2D FE model of the experimental setup is used to simulate the same axial strain distribution and a least-squares error function is generated on this basis. The bridging tractions are represented by a user-defined exponential function-based pressure distribution (completely defined by three model parameters), which acts along the cracked surface of the DCB specimen. Optimisation schemes are applied to identify the model parameters, and the resulting bridging traction distribution is converted to a bridging law by post-processing (Sorensen et al., 2007).

The bridging laws obtained by the inverse approach in (Sorensen et al., 2007) is compared to the J-integral approach in (Sorensen et al., 2008). The two approaches are shown to provide similar bridging laws. However, the J-integral approach is observed to be sensitive to the value of the critical separation, δ_c, which requires an educated selection by the user.

This section has provided a brief introduction to different direct and inverse approaches for characterisation of cohesive laws. An inverse method for parameter identification of spline-based cohesive laws with a large number of model parameters is developed in paper B. A comparison of the inverse
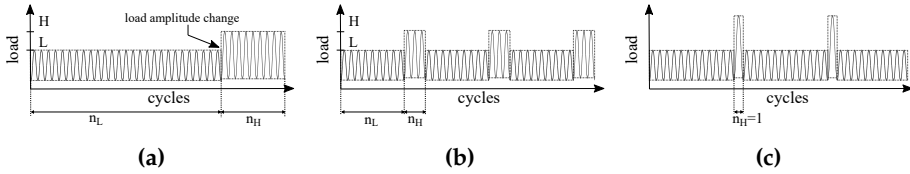
Fig. 2.4: Common load events responsible for load interaction effects. (a) Load sequencing (in LH sequence). (b) Frequent mixing of load blocks (i.e. cycle-mixing). (c) Infrequent overload events.

method and the J-integral approach is also provided in paper B.

2.2 Fatigue in FRP composites under VA loading

2.2.1 Load interaction effects and fatigue damage

The majority of the experimental studies in the current section consider fatigue damage in terms of specimen lifetime and degradation of macroscopic specimen properties (e.g. residual strength and/or residual stiffness). Fatigue-driven delamination and fatigue crack growth of single cracks in FRP composite materials will be considered in the following section, Sec. 2.2.2.

It is well established that the fatigue damage accumulation in FRP composite materials is sensitive to load interaction effects (Broutman and Sahu, 1972; Heath Smith, 1979; Yang and Jones, 1981; Hwang and Han, 1986; Schaff and Davidson, 1997a,b; Bartley-Cho et al., 1998; Farrow, 1998). However, many models and experimental observations in the literature concerning load interaction effects have been established for laminates with a particular laminate architecture, boundary conditions, testing conditions, VA load pattern etc. which makes it difficult to assess the generality of the results (Van Paepegem and Degrieck, 2002).

Experimental studies of VA loading typically apply one of the three following characteristic load spectra: I) A block loading spectrum that consists of two or more CA blocks with different amplitude and mean values, e.g. (Schaff and Davidson, 1997a; Bartley-Cho et al., 1998). II) Standardized in-service load spectra, e.g. the FALSTAFF load spectrum (Heath Smith, 1979; Schaff and Davidson, 1997b; Filis et al., 2004). III) A stochastic load spectrum generated based on a prescribed distribution of fatigue loads, e.g. (Himmel, 2002). The experimental studies of fatigue in FRP composites under VA loading have revealed several load events that are prone to cause load interaction effects. Some of the most common load events are illustrated in Fig. 2.4.

The load sequence effect is often investigated by varying the sequence of high- (H) and low (L) load blocks as illustrated in Fig. 2.4(a). A brief literature review on load sequence effects in laminated FRP composite materials

is provided in (Van Paepegem and Degrieck, 2002), which concludes that the opinions in the literature on the most damaging load sequence is strongly divided.

An example of the load sequence effect is highlighted here. Load sequence effects in carbon/epoxy cross-ply laminates are investigated using in-plane tension-tension fatigue tests in (Gamstedt and Sjögren, 2002). The high-to-low sequence results in shorter fatigue lifetimes than the opposite load sequence. The authors in (Gamstedt and Sjögren, 2002) emphasise that the observed load sequence effect is a consequence of the interaction between the initiatory damage mechanism, e.g. transverse matrix cracks that dominate at high load levels, and the progressive damage mechanism, e.g. delamination growth that dominates at low load levels, as illustrated in Fig. 2.5. The transverse matrix cracks serve as places of initiation for delamination, but delamination tends to suppress further transverse cracking. Conclusively, the authors in (Gamstedt and Sjögren, 2002) state that the load sequence effect in arbitrary laminated composite materials can be explained with similar physical arguments on the initiatory and progressive damage mechanisms.

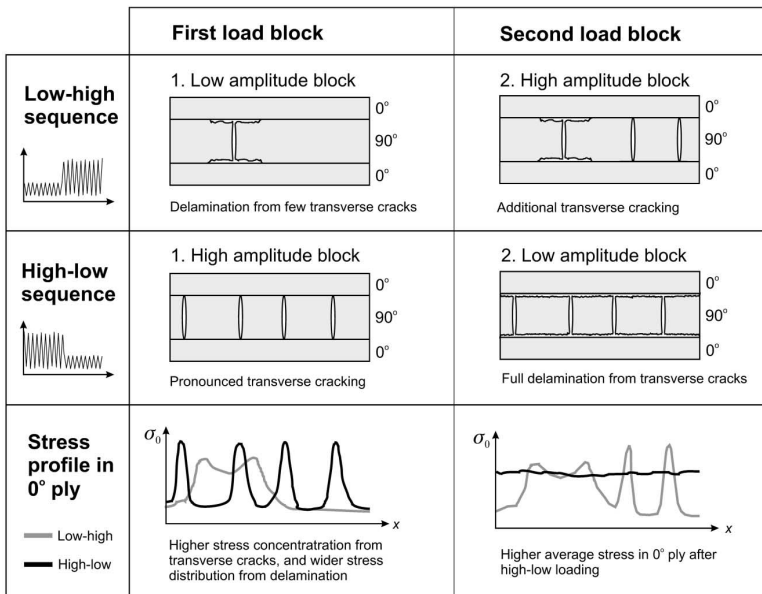When frequent changes in load amplitude occur (i.e. frequent mixing of

Fig. 2.5: Schematic illustration of the evolution of damage and the load sequence effect in block amplitude loading of CFRP cross-ply laminates, and the qualitative influence on the stress profile in the critical 0° plies. Reprinted from (Gamstedt and Sjögren, 2002) with permission from publisher Elsevier ©.

load cycles), a so-called cycle-mix effect becomes more critical than the load sequence effect (Farrow, 1998, 1996). The cycle-mix effect is typically investigated using two-level block loading as illustrated in Fig. 2.4(b). Laminates that experience repeated L- and H-load blocks of short duration (e.g. $n_L = 1000$ and $n_H = 10$ cf. Fig. 2.4(b) such that $n_L/n_H = 100$) have reduced average lifetime as compared to laminates that are subjected to repeated L- and H-load blocks of long duration (e.g. $n_L = 100000$ and $n_H = 1000$ such that $n_L/n_H = 100$). This is in spite the fact that the ratios of high and low load cycles (n_H/n_L) are kept the same in both cases. The cycle-mix effect is originally studied in (Farrow, 1998), wherein notched ("fastener type") specimens, which are made of ± 45 angle-ply and quasi-isotropic carbon/epoxy laminates, are subjected to load patterns similar to Fig. 2.4(b) under uni-axial cyclic loading.

The cycle-mix effect in laminated FRP composite materials has been discussed in several investigations (Schaff and Davidson, 1997a,b; Filis et al., 2004; Van Paepegem and Degrieck, 2002). For example, a cycle-mix factor is introduced in a residual strength model in the work by (Schaff and Davidson, 1997a,b). The cycle-mix factor reduces the residual strength and is applied (only) when the magnitude of the mean stress increases from one load segment to the next. Predictions from the residual strength model in (Schaff and Davidson, 1997a) are compared to the cycle-mix experiments from (Farrow, 1998). The predictions are improved significantly by inclusion of the cycle-mix factor (Schaff and Davidson, 1997a). The same model provides good predictions of the fatigue-life in similar specimens subjected to the standardised FALSTAFF load spectrum in (Schaff and Davidson, 1997b). This result highlights the importance of taking load amplitude changes into consideration when modelling fatigue under real load spectra.

To accomplish fatigue modelling for generalised loading and arbitrary laminate architectures, a mechanistic approach, which quantitatively accounts for the progression of actual damage mechanisms (e.g. matrix cracking, delamination), is necessary (Talreja, 2000; Degrieck and Van Paepegem, 2001; Gamstedt and Sjögren, 2002). Then similar physical reasoning as in (Gamstedt and Sjögren, 2002) (concerning load sequence effects in cross-ply laminates) can be applied to explain load interaction effects in general. In this regard, a quote from (Gamstedt and Sjögren, 2002) is highlighted, which concerns a mechanistic approach to fatigue under VA loading: "*The key is to (i) identify the damage mechanisms at different stress amplitudes, (ii) quantify their kinetics in fatigue, (iii) relate their interaction by stress analysis, and (iv) conceive a failure criterion. . . . If the underlying mechanisms, their kinetics and mutual interaction, have been well characterized, the fatigue lifetime of an arbitrary lay-up subjected to an arbitrary load history can be predicted.*".

Experimental research that measures the progression of the actual delam-

ination growth in fatigue under VA loading is of high interest in this regard. This is the topic of the following section and papers C-D.

2.2.2 Fatigue-driven delamination growth under VA loading

Load interaction effects in fatigue-driven delamination growth is an area of little experimental research. One of the few experimental works considering load interaction effects in interlaminar cracking is (Erpolat et al., 2004) where CFRP laminates are tested using the conventional mode I DCB test, see Fig. 1.9(b). DCB specimens are subjected to intermittent overload events every 20th load cycle (in a similar manner as illustrated in Fig. 2.4(c)), using two-level block amplitude loading under displacement-control. The results in (Erpolat et al., 2004) show an accelerated crack growth in comparison to estimates based on CA data obtained using numerical crack growth integration (similar to Eq. (1.7)) and Paris' law-like relations. The authors in (Erpolat et al., 2004) suggest that the overload events create a damage zone ahead of the crack tip, which decreases the resistance to crack growth and enables the damage to progress at a significantly higher rate in the subsequent load cycles.

Another study investigates the influence of a low-to-high (LH) load sequence on the mode I delamination growth in UD CFRP laminates (Yao et al., 2016b) using the conventional DCB test configuration. The results show an increased crack growth rate due to the LH load sequence in comparison to a CA base-line test. The LH load sequence shifts the fatigue resistance curve $(\Delta G, da/dN)$ to the left such that a higher crack growth rate, da/dN, occurs for a given ERR range, ΔG. The authors in (Yao et al., 2016b) suggest that more bridging fibres can be generated in the wake of the crack tip during a high load block compared to the amount of bridging fibres generated during the low load block. This difference in the amount of fibre bridging can finally cause the shift of the fatigue resistance curve. This suggests that fibre bridging can be one of the main responsible mechanisms for load interaction effects in fatigue-driven delamination.

The effect of fibre bridging on fatigue-driven delamination in laminated FRP composite materials is investigated in several works, and there is general consensus that fibre bridging reduces the fatigue crack growth rate (Hwang and Han, 1989; Hojo et al., 1995; Yao et al., 2014; Donough et al., 2015; Yao et al., 2016a; Farmand-Ashtiani et al., 2016; Yao et al., 2017b,a). The effect of fibre bridging on the fatigue resistance curves $(\Delta G, da/dN)$ is investigated in (Yao et al., 2014) using the conventional DCB specimen subjected to CA loading under displacement-control. A series of $(\Delta G, da/dN)$-curves is generated with different amount of fibre bridging by following a specific test procedure to generate quasi-static crack extensions of different length prior to the fa-

tigue tests. Additionally, it is assumed that the amount of bridging fibres in the wake of the crack tip is related to the crack length. It is found that the longer the crack (i.e. the more bridging fibres in the crack wake), the further the fatigue resistance curves shift from left to right (i.e. a higher fatigue crack growth resistance) (Yao et al., 2014). In terms of Paris-like relations, it appears that the exponent n, cf. Eq. (1.6), remains independent of the amount of fibre bridging, however, the parameter C, cf. Eq. (1.6), depends significantly on the amount of fibre bridging (Yao et al., 2016a).

Experimental research on fatigue-driven delamination growth under VA loading in laminated FRP composite materials is limited. Nevertheless, a few similar studies on fatigue crack growth in adhesively bonded FRP composite joints under VA loading may be relevant to include here. Load interaction effects during fatigue crack growth in adhesively bonded CFRP laminates is compared to the interlaminar crack growth in CFRP laminates using the conventional mode I DCB test in (Erpolat et al., 2004). The DCB specimens are subjected to two-level block amplitude loading with intermittent overload events, as explained in the beginning of the current section. The adhesive cracking and interlaminar crack tests both show a discrepancy with respect to predictions based on CA data and a simple non-interaction model. The fatigue crack growth in the adhesively bonded DCB specimens is slightly underestimated, however, in the case of interlaminar fatigue cracking, the CA predictions is even more non-conservative (Erpolat et al., 2004). Thus, the load interaction effect is more pronounced in the fatigue interlaminar cracking (delamination) DCB tests in comparison to the fatigue crack growth in the adhesively bonded DCB tests (Erpolat et al., 2004).

Fatigue crack growth and load interaction effects in adhesively bonded pultruded GFRP joints is investigated under block amplitude loading in (Sarfaraz et al., 2013a) and the WISPERX load spectrum in (Sarfaraz et al., 2013b; Vassilopoulos, 2015) using the double lap joint specimen. A load sequence effect is observed, which may accelerate or retard the crack growth depending on the load sequence. Under tensile loading of the double lap joint a crack growth acceleration is observed due to the LH load sequence, whereas the opposite load sequence (HL) causes crack growth retardation (Sarfaraz et al., 2013a). Additionally, fibre bridging is observed to contribute to the fracture process. The authors suggest that the acceleration during the LH load sequence is attributed to significant breakage of bridging fibres during the load amplitude change, which causes a lower fracture resistance and a higher crack growth rate in subsequent load cycles (Sarfaraz et al., 2013a). The cycle-mix effect in two-level block amplitude loading is also investigated in (Sarfaraz et al., 2013a) by analysis of the fatigue lifetime. The frequent changes in load amplitude is shown to significantly decrease the fatigue lifetime (even more than the load sequence effect), however, no measurements of

the actual fatigue crack growth behaviour during the cycle-mix experiment is available (Sarfaraz et al., 2013a).

2.3 Summary of literature review

The literature review presented in this chapter has revealed numerous publications relevant to the two major topics of the current work: I) Cohesive zone modelling of quasi-static delamination with large-scale fibre bridging and characterisation of advanced cohesive laws. II) Fatigue-driven delamination under VA loading and load interaction effects. A brief summary of the literature review is provided here.

An advanced CZM is necessary when large-scale fibre bridging prevails in the wake of a delamination crack tip. To accurately account for large-scale fibre bridging the cohesive law must be able to represent the bridging mechanism, among others, which is often associated with complex shapes of the cohesive law (i.e. *advanced* cohesive laws). The advanced cohesive laws require additional cohesive parameters in comparison to the conventional cohesive laws, e.g. the bilinear cohesive law. This naturally complicates the characterisation of traction-separation relations. Several advanced cohesive laws are available in the literature; especially the trilinear cohesive law is popular to account for fibre bridging. However, other advanced cohesive laws, e.g. mixed-mode capable spline-based cohesive laws, possess interesting and unexploited properties with respect to delamination modelling in laminated FRP composite materials for several reasons as given in Sec. 2.1.2.

The fatigue damage accumulation in laminated FRP composite materials is sensitive to load interaction effects. Load sequencing, cycle-mixing and overloads are frequently occurring load events in real load spectra that are likely to cause load interaction effects. The usual damage metrics applied in experimental research on VA loading of laminated FRP composite materials is the number of load cycles to failure, or the degradation of macroscopic specimen properties (e.g. the specimen's residual strength or residual stiffness). However, experimental research on the progression of the actual specific damage (e.g. matrix cracking and delamination) under VA loading is limited. Very few works consider fatigue-driven delamination under VA loading. Experimental research on the progression of the actual delamination growth behaviour during VA loading is important to develop delamination prediction models that account for load interaction effects. Several publications prove that bridging fibres reduce the fatigue crack growth rate, and few studies suggest that fibre bridging contributes to load interaction effects. However, there are neither experimental observations nor a clear consensus on the actual role of bridging fibres with respect to load interaction effects.

Finally, delamination prediction models are most often based on non-interaction models and CA data, which yields highly non-conservative predictions, and the limitations of such assumptions is currently unknown.

3

Summary of Papers

The chapter presents papers A-D and provides a summary of results. The papers have been published in peer-reviewed international scientific journals. An overview of the papers are provided in a previous section, "*Primary Publications in Journals*". Papers A-B are concerned with CZM of quasi-static delamination with large-scale fibre bridging. Papers C-D are experimental works concerned with fatigue-driven delamination under VA loading. Finally, the scientific contributions and impact of the papers are discussed.

3.1 Paper A:

Title: "*Formulation of a mixed-mode multilinear cohesive zone law in an interface finite element for modelling delamination with R-curve effects*". Paper A (Jensen et al., 2019b) presents a linear spline-based cohesive law with an arbitrary number of line segments (i.e. multilinear) capable of simulating mixed-mode cracking. The mixed-mode multilinear cohesive law is an equivalent one-dimensional formulation and implemented in an intrinsic interface finite element through user-programmable features in Ansys Mechanical. The main focus of the paper is constitutive damage modelling, including a novel damage model, crack mode interpolation functions, a constitutive tangent stiffness tensor, and application of such to simulate delamination with fibre bridging. Single interface element verification studies of the mixed-mode multilinear cohesive law formulation are conducted under mixed-mode crack opening. The interface element is applied in a FE model to simulate quasi-static mode I delamination with large-scale fibre bridging in a pure moment loaded DCB specimen made of a UD glass/epoxy laminate. The multilinear cohesive law simulates the R-curve behaviour in excellent agreement with experimental measurements. The simulated response obtained from a multilinear cohesive law with 15 line segments is compared to the simulated responses obtained from bilinear and trilinear cohesive laws. The comparison demonstrates that complex traction-separation relations can be necessary to

obtain accurate simulations of R-curve behaviour, and that the linear spline-based cohesive law gives a lot of insight to the actual variation of cohesive tractions with crack opening displacement.

3.2 Paper B:

Title: "*Inverse parameter identification of n-segmented multilinear cohesive laws using parametric finite element modelling*". Paper B (Jensen et al., 2019a) presents a methodology to measure advanced parametric cohesive laws based on inverse analysis using FEM and gradient-based optimisation. A delamination experiment is simulated with a parametric FE model, which utilises the interface element formulation in paper A (Jensen et al., 2019b) having a parametric representation of the multilinear cohesive law. To identify the cohesive parameters, a gradient-based optimisation procedure iteratively varies the cohesive parameters to minimise an error function in terms of structural responses measured from an experiment and a FE model. The methodology is applied to identify multilinear cohesive laws from a quasi-static test on a mode I pure moment loaded DCB specimen made of a glass/epoxy laminate. A residual vector is defined from the difference in global response curves (measurements of the applied bending moment and angle of rotation at the crack mouth of the DCB) between the FE model and the experiment. A non-linear least squares formulation of the residual vector defines the objective function, which is minimised using a gradient-based optimisation algorithm. The cohesive parameters of the multilinear cohesive law has been identified when the optimisation algorithm converges to an optimal solution. The inverse methodology is shown to be robust in obtaining identical optimal solutions independent of the initial guess and other settings in the methodology. The simulation reproduce the experimental data with good agreement on global (i.e. specimen) level and local (i.e. crack tip) level. Parametric studies related to the number and distribution of line segments in the multilinear cohesive law is conducted. Finally, the solutions obtained with the inverse method is compared to solutions based on the J-integral approach.

3.3 Paper C:

Title: "*Transition-behaviours in fatigue-driven delamination of GFRP laminates following step changes in block amplitude loading*". Paper C (Jensen et al., 2021a) is concerned with experimental characterisation and understanding of load interaction effects and fibre bridging in fatigue-driven delamination under variable amplitude loading. The paper presents experimental results from a test campaign using the conventional DCB test configuration, see Fig. 1.9(b), under displacement-controlled two-level block amplitude loading. A recently

developed digital image-based method for automated tracking of delamination fronts in translucent materials is utilised which enables precise measurements of the crack extension. CA base-line tests are compared to block loading tests in a low-to-high (LH) and high-to-low (HL) load sequence. Emphasis is put on the crack growth behaviour following the step change in load amplitude from one load block to another. For example, the crack growth rate following the change from a low load block to a high load block. The experimental results are analysed in terms of the crack growth rate, the crack extension, and the ERR. A load amplitude change in the LH load sequence causes an immediate increase in the crack growth rate, which is several times higher than the crack growth rate in the CA base-line test. The crack growth rate remains higher than the CA base-line test for a significant amount of further crack extension before it reaches a crack growth rate similar to the base-line. In the opposite load sequence, the HL load amplitude change causes retardation of the crack growth. The observed transition-behaviours of the crack growth rate following the load amplitude changes are non-negligible, however, currently ignored in state-of-the-art crack growth rate models for prediction of fatigue-driven delamination. The results should motivate further research.

3.4   Paper D:

Title: "*Transient delamination growth in GFRP laminates with fibre bridging under variable amplitude loading in G-control*". In paper D (Jensen et al., 2021b) a novel test rig is applied to investigate mode I fatigue-driven delamination growth under VA loading in G-control (ERR-control). The test rig utilises the pure moment loaded DCB test configuration which possesses several advantages over the conventional DCB test with respect to large-scale fibre bridging, steady-state crack growth, G-control testing, and VA loading. The DCB specimens are subjected to two-level block amplitude loading in G-control. The applied VA load patterns consist of single- and periodic load amplitude changes (see Fig. 2.4(b)). The cycle-mix effect is investigated by varying the frequency of the periodic load amplitude changes. A transient crack growth response is observed to occur due to every load amplitude change under consideration. The crack growth rate in the transient response is significantly different from CA base-line tests. The crack growth rate following a certain load amplitude change depends on the load history. Increasing the frequency of periodic load amplitude changes accelerates the crack growth even further. For example, in a simple VA load pattern of 10 periodic repeated L- and H-load blocks (see Fig. 2.4(b)) the delamination has extended a factor of 2.2 times the delamination extension predicted based on CA data and non-interaction models.

3.5 Contributions and impact

Contributions and impact of the work in papers A-D are highlighted in the current section. Papers A-B are concerned with new methods for simulation of quasi-static delamination in laminated FRP composite materials experiencing large-scale fibre bridging. The cohesive law must be able to account for several co-existing damage mechanisms that act at different length scales in the FPZ. This requires advanced cohesive laws, and particularly spline-based cohesive laws possess several interesting and unexploited properties in this regard, as argued in Sec. 2.1.2. To the author's knowledge the mixed-mode multilinear cohesive law in paper A is among the first spline-based mixed-mode capable cohesive laws available in the literature. The multilinear cohesive law possesses a high degree of freedom such that any shapes of the softening traction-separation relation can be achieved. Additionally, the multilinear cohesive law reduces a priori shape assumptions and yields an accurate representation of the cohesive tractions.

Generally, the spline-based cohesive laws require a relatively high number of model parameters. Few works in the literature consider inverse parameter identification of spline-based cohesive laws (Shen et al., 2010; Shen and Paulino, 2011; Xu et al., 2017; Pereira et al., 2017, 2018). The work in paper B is a new application of such to laminated FRP composite materials with large-scale fibre bridging. The inverse method in paper B is shown to be an efficient and robust methodology to identify model parameters of multilinear cohesive laws using gradient-based optimisation - even for a high number of model parameters.

The models and characterisation methods developed in paper A-B are useful tools in damage tolerant design approaches. One primary contribution in paper A is the novel constitutive damage model in the CZM framework. The mixed-mode multilinear cohesive law is implemented in the commercial FE code ANSYS Mechanical (implicit FEA) as an interface element through user-programmable features. This makes the present CZM widely applicable in academia and industry.

The characterisation methodology in paper B (in combination with the CZM in paper A) can be applied to develop and optimise damage tolerant materials, e.g. materials that possess increasing fracture resistance with increasing crack extension due to fibre bridging. A few examples are provided here. The more degrees of freedom in the traction-separation relation, the higher the sensitivity becomes to measure the influence of certain conditions on the shape of the cohesive law. This may be of interest with respect to micro-structural optimisation. For example, the fracture energy of the fibre/matrix interface at a microscopic level will influence the fibre bridging

mechanisms and hence the shape of the cohesive law. The methods may also be important in many industries in order to assess the effect of in-service environmental conditions on the shape of the cohesive law. For example, wind turbine blades and automotive components operate under a wide range of temperatures and moisture contents which may deteriorate the interface fracture toughness and the fibre bridging mechanisms.

The tools developed in paper A-B are not limited to delamination problems in laminated FRP composite materials but applicable to many fracture problems across different fields in engineering and science. The tools apply to material systems with arbitrary softening traction-separation relations, for example, concrete-like materials and biological tissue, which also have complex FPZs.

Papers C-D are concerned with fatigue-driven delamination in laminated FRP composite materials under VA loading. This is a field of limited experimental research and many unsolved problems, as described in Sec. 2.2.2. To the author's knowledge the fatigue crack growth rate of delaminations in laminated FRP composite materials has not previously been investigated to the extend here. Special attention is given to the transient crack growth rate following the load amplitude changes and the influence of the load history on the current crack growth rate. The experimental campaign in paper C takes point of departure in the conventional DCB test specimen subjected to simple two-level block amplitude loading with focus on a single load amplitude change. Paper C shows a potential for further analysis of the crack growth behaviour following load amplitude changes. This is pursued in paper D considering more complex VA load patterns using a refined experimental setup.

Paper D applies the pure moment loaded DCB test configuration for G-controlled cyclic testing. To the author's knowledge, this has not previously been applied to study fatigue-driven delamination in laminated FRP composite materials with large-scale FPZs. The pure moment loaded DCB test configuration is specially convenient for analysis of load interaction effects in fatigue-driven delamination for several reasons, which are not achievable in the conventional force- or displacement-controlled DCB test. A few advantageous properties of the pure moment loaded DCB specimen for cyclic testing are mentioned here (Suo et al., 1992; Bao and Suo, 1992; Sørensen and Jacobsen, 2000): *(I)* The J-integral of the pure moment loaded DCB specimen is independent of the crack length and the magnitude and distribution of tractions in the FPZ (under small- as well as large-scale FPZ conditions). *(II)* No corrections for shear or beam root rotation effects are necessary. *(III)* The pure moment loaded DCB specimen is a steady-state specimen. Additional properties of the test configuration are provided in paper D.

The pure moment loaded DCB test configuration is rarely applied in fatigue, however, the aforementioned properties (*I-III*) makes the test config-

uration highly suited for investigation of other unsolved research problems. For example, characterisation of the effect of fibre bridging on fatigue-driven delamination (see Sec. 2.2.2) and how to account for fibre bridging in crack growth rate models. In that sense, the experimental methodology in paper D may give inspiration for new characterisation methods in fatigue-driven delamination with large-scale fibre bridging - or fatigue crack growth in other materials with a large-scale FPZ in general.

State-of-the-art models for prediction of fatigue-driven delamination assume that the current crack growth rate is a function of the instantaneous ERR and that any load interaction effects are negligible (Bak et al., 2014). This is highly contradictory to the results in paper C-D. A simple example is included in paper D, where a non-interaction model based on CA data are shown to significantly under-estimate the actual delamination extension when frequent load amplitude changes occur. The damaging effect of frequent load amplitude changes in fatigue-driven delamination and the associated crack growth behaviour is an important finding in this regard. Additionally, the experimental measurements in paper D of the crack growth rate during G-controlled VA load patterns may be useful as benchmark problems for future crack growth rate models that attempt to incorporate load interaction effects.

References

Abdel-Monsef SA, Renart J, Turon A, Maimí P (2019) Formulation of a cohesive zone model with humidity and temperature effects for modelling bonded joints. In: 7th ECCOMAS Thematic Conference on the Mechanical Response of Composites: COMPOSITES2019 (book of abstracts)

Abdel-Monsef SA, Renart J, Carreras L, Maimí P, Turon A (2020) Effect of environmental conditioning on pure mode i fracture behaviour of adhesively bonded joints. Theoretical and Applied Fracture Mechanics 110:102826

Aicher W, Branger J, van Dijk GM, Ertelt J, Hück M, de Jonge JB, Lowak H, Rhomberg H, Schütz D, Schütz W (1976) Description of a fighter aircraft loading standard for fatigue evaluation FALSTAFF. Tech. rep., Common report of F+W Emmen, LBF, NLR, IABG

Airoldi A, Dávila CG (2012) Identification of material parameters for modelling delamination in the presence of fibre bridging. Composite Structures 94 (11):3240–3249

Albertsen H, Ivens J, Peters P, Wevers M, Verpoest I (1995) Interlaminar fracture toughness of cfrp influenced by fibre surface treatment: Part 1. experimental results. Composites Science and Technology 54:133–145

Alfano G (2006) On the influence of the shape of the interface law on the application of cohesive-zone models. Composites Science and Technology 66(6):723–730

Alfano G, Crisfield MA (2001) Finite element interface models for the delamination analysis of laminated composites: mechanical and computational issues. Int J Numer Meth Eng 50(7):1701–1736

Alfano M, Lubineau G, Paulino GH (2015) Global sensitivity analysis in the identification of coheisve models using full-field kinematic data. International Journal of Solids and Structures

Allix O, Ladevéze P, Corigliano A (1995) Damage analysis of interlaminar fracture specimens. Composite Structures 31:61–74

Anthony J, Paris PC (1988) Instantaneous evaluation of j and c*. International Journal of Fracture 38:R19–R21

Bak BLV (2015) Progressive damage simulation of laminates in wind turbine blades under quasistatic and cyclic loading. PhD thesis, Aalborg Universitetsforlag, Ph.d.-serien for Det Teknisk-Naturvidenskabelige Fakultet, Aalborg Universitet

Bak BLV (2017) Lecture notes: Fracture mechanics for laminated composite structures. lecture notes, Department of Materials and Production

Bak BLV, Sarrado C, Turon A, Costa J (2014) Delamination under fatigue loads in composite laminates: A review on the observed phenomenology and computational methods. Applied Mechanics Reviews 66:1–24

Bao G, Suo Z (1992) Remarks on crack-bridging concepts. Appl Mech Rev 45, 8:355 – 366

Barenblatt GI (1959) Concerning equilibrium cracks forming during brittle fracture: the stability of isolated cracks. J Appl Math Mech 23:622–636

Barenblatt GI (1962) The mathematical theory of equilibrium cracks in brittle fracture. In: Advances in Applied Mechanics, Academic Press, New York 7:55–129

Bartley-Cho J, Lim SG, Hahn HT, Shyprykevich P (1998) Damage accumulation in quasi-isotropic graphite/epoxy laminates under constant-amplitude fatigue and block loading. Composites Sci Technol 58:1535–1547

Benzeggagh ML, Kenane M (1996) Measurement of mixed-mode delamination fracture toughness of unidirectional glass/epoxy composites with mixed-mode bending apparatus. Composites Science and Technology 56:439–449

Bouhala L, Makradi A, Belouettar S, Younes A, Natarajan S (2015) Composite laminate delamination simulation and experiment: A review of recent development. Computers and Structures 153:91–97

Broutman LJ, Sahu S (1972) A new theory to predict cumulative fatigue damage in fiberglass reinforced plastics. Composite Materials Testing and Design, ASTM STP 497 pp 170–88

Camacho GT, Ortiz M (1996) Computational modelling of impact damage in brittle materials. International Journal of Solids and Structures 33(20-22):2899–2938

Camanho PP, Dávila CG, de Moura MF (2003) Numerical simulation of mixed-mode progressive delamination in composite materials. J Compos Mater 37(16):1415–1438

Carreras L, Lindgaard E, Renart J, Bak BLV, Turon A (2019) An evaluation of mode-decomposed energy release rates for arbitrarily shaped delamination fronts using cohesive elements. Computer Methods in Applied Mechanics and Engineering 347:218–237

Chen BY, Tay TE, Pinho ST, Tan VBC (2016) Modelling the tensile failure of composites with the floating node method. Computer Methods in Applied Mechanics and Engineering 308:411–442

Chen J, Crisfield M, Kinloch A, Busso E, Matthews F, Qui Y (1999) Predicting progressive delamination of composite material specimens via interface elements. Mechanics of Composite Materials and Structures 6:301–317

Cox BN, Marshall DB (1991) The determination of crack bridging forces. International Journal of Fracture 49:159–176

Daneshjoo Z, M SM, Fakoor M (2018) A micromechanical model for prediction of mixed mode i/ii delamination of laminated composites considering fiber bridging effects. Theoretical and applied fracture mechanics 94:46–56

Degrieck J, Van Paepegem W (2001) Fatigue damage modeling of fibre-reinforced composite materials: Review. Applied Mechanics Reviews 54(4):279–300

Djursing T (2021) Overbefolkning er et monster i klimakampen. Ingeniøren 5:1,4–5

Donough MJ, Gunnion AJ, Orifici AC, Wang CH (2015) Scaling parameter for fatigue delamination growth in composites under varying load ratios. Composites Science and Technology 120:39–48

Dugdale DS (1960) Yielding of steel sheets containing slits. J Mech Phys Solids 8(2):100–104

Dávila CG, Rose CA, Camanho PP (2009) A procedure for superposing linear cohesive laws to represent multiple damage mechanicsms in the fracture of composites. International Journal of Fracture 158:211–223

Elices M, Guinea GV, Gómez J, Planas J (2002) The cohesive zone model: advantages, limitations and challenges. Engineering Fracture Mechanics 69:137–163

Erpolat S, Ashcroft IA, Crocombe AD, Abdel-Wahab MM (2004) Fatigue crack growth acceleration due to intermittent overstressing in adhesively bonded cfrp joints. Composites Part A: Applied Science and Manufacturing 35:1175–1183

Farmand-Ashtiani E, Cugnoni J, Botsis J (2014) Specimen thickness dependence of large scale fiber bridging in mode i interlaminar fracture of carbon epoxy composites. International Journal of Solids and Structures 55:58–65

Farmand-Ashtiani E, Cugnoni J, Botsis J (2016) Effects of large scale bridging in load controlled fatigue delamination of unidirectional carbon-epoxy specimens. Composites Science and Technology 137:52–59

Farrow IR (1996) Fatigue of composite materials under aircraft service loading. Technical note, proc inst mech engrs vol 210, Department of Aerospace Engineering, University of Bristol

Farrow IR (1998) Damage accumulation and degradation of composite laminates under aircraft service loading: Assessment and prediction, volumes i and ii. PhD thesis, Cranfield Institute of Technology

Filis PA, Farrow IR, Bond IP (2004) Classical fatigue analysis and load cycle mix-event damage accumulation in fibre reinforced laminates. Int J Fatigue 26:565–573

Gamstedt EK, Sjögren BA (2002) An experimental investigation of the sequence effect in block amplitude loading of cross-ply composite laminates. Int J Fatigue 24:437–446

Gowrishankar S, Mei H, Liechti MK, Huang R (2012) A comparison of direct and iterative methods for determining traction-separation relations. Int J Fract 177:109–128

Goyal VK, Johnson ER, Dávila CG (2004) Irreversible constitutive law for modeling the delamination process using interfacial surface discontinuities. Composite Structures 65:289–305

Grytten F, Sørensen BF, Goutianos S, Joki RK, Jørgensen JK (2020) D1.1 Micromechanical model for fibre peel-off and pull-out. Tech. rep., SINTEF, DACOMAT project, No. 761072

Hashemi S, Kinloch AJ, Williams JG (1989) Corrections needed in double cantilever beam tests for assessing the interlaminar failure of fiber composites. Journal of Materials Science Letters 8:125–129

Hashemi S, Kinloch AJ, Williams JG (1990a) The analysis of interlaminar fracture in uniaxial fibre-polymer composites. Proc R Soc Lond A 427:173–199

Hashemi S, Kinloch AJ, Williams JG (1990b) Mechanics and mechanisms of delamination in a poly(ether sulphone)-fiber composite. Composites Science and Technology 37:429–462

ten Have AA (1992) WISPER and WISPERX - final definition of two standardised fatigue loading sequences for wind turbine blades. Tech. rep., NLR-Report CR 91476 U, Amsterdam

Heath Smith JR (1979) Theoretical considerations in the use of FALSTAFF loading for fatigue research in carbon fibre composite. Tech. rep., RAe TR 79124

Heidari-Rarani M, Shokrieh MM, Camanho PP (2013) Finite element modelling of mode i delamination growth in laminated dcb specimens with r-curve effects. Composites: Part B 45:7

Heuler P, Klätschke H (2005) Generation and use of standardised load spectra and load-time histories. Int J Fatigue 27:974–990

Hillerborg A, Modéer M, Petersson PE (1976) Analysis of crack formation and crack growth in concrete by means of fracture mechanics and finite elements. Cement and Concrete Research 6(6):773–781

Himmel N (2002) Fatigue life prediction of laminated polymer matrix composites. International Journal of Fatigue 24:349–360

Hojo M, Ochiai S, Aoki T, Ito H (1995) Mode i fatigue delamination for cf/peek laminates using maximum-energy-release-rate constant tests. J Soc Mat Sci Japan 44 (502):953–959

Huber O, Nickel J, Kuhn G (1993) On the decomposition of the j-integral for 3d crack problems. International Journal of Fracture 64:339–348

Hutchinson JW, Suo Z (1992) Mixed mode cracking in layered materials. Advances in applied mechanics 29:63–191

Hwang W, Han KS (1986) Cumulative damage models and multi-stress fatigue life prediction. Journal of Composite Materials 20:125–153

Hwang W, Han KS (1989) Interlaminar fracture behaviour and fiber bridging of glass-epoxy composite under mode i static and cyclic loadings. Journal of Composite Materials 23:396–430

Ivens J, Albertsen H, Wevers M, Verpoest I, Peters P (1995) Interlaminar fracture toughness of cfrp influenced by fibre surface treatment: Part 2. modelling of the interface effect. Composites Science and Technology 54:147–159

Jensen PH, Fugleberg K (2015) Wind energy research strategy. report, Danish Research Consortium for Wind Energy, www.DFFV.dk

Jensen SM, Martos MJ, Bak BLV, Lindgaard E (2019a) Formulation of a mixed-mode multilinear cohesive zone law in an interface finite element for modelling delamination with r-curve effects. Composite Structures 216:477 – 486, DOI https://doi.org/10.1016/j.compstruct.2019.02.029

Jensen SM, Martos MJ, Lindgaard E, Bak BLV (2019b) Inverse parameter identification of n-segmented multilinear cohesive laws using parametric finite element modeling. Composite Structures 225:111074, DOI https://doi.org/10.1016/j.compstruct.2019.111074

Jensen SM, Bak BLV, Bender JJ, Lindgaard E (2021a) Transition-behaviours in fatigue-driven delamination of gfrp laminates following step changes in block amplitude loading. International Journal of Fatigue 144:106045, DOI https://doi.org/10.1016/j.ijfatigue.2020.106045

Jensen SM, Bak BLV, Carreras L, Bender JJ, Lindgaard E (2021b) Transient delamination growth in gfrp laminates with fiber bridging under variable amplitude loading in g-control. *submitted*

Jones RM (1999) Mechanics of Composite Materials, second edition edn. Taylor and Francis

Katnam KB, Sargent JP, Crocombe AD, Khoramishad H, Ashcroft IA (2010) Characterization of moisture-dependent cohesive zone properties for adhesively bonded joints. Engineering Fracture Mechanics 77 (16):3105–3119

Kaute DAW, Shercliff HR, Ashby MF (1993) Delamination, fiber bridging and toughness of ceramic matrix composites. Acta Metall Mater 41:1959–1970

Köhler M, Jenne S, Pötter K, Zenner H (2017) Load assumptions for fatigue design of structures and components - counting methods, safety factors, practical applications. Springer

Krueger R (2002) The virtual crack closure technique: History, approach and applications. NASA/CR-2002-211628

Krueger R (2011) Development of benchmark examples for static delamination propagation and fatigue growth predictions. Tech. rep., Langley Research Center, Technical Report No. NASA/NF-1676L-11493

Li VC, Ward RJ (1989) A novel testing technique for post-peak tensile behaviour of cementitious materials. In: Mishashi H, Takahashi H, Wittmann FH, editors Fracture toughness and fracture energy - testing methods for concrete and rocks Rotterdam: AA Balkema Publishers pp 183–195

Lindgaard E, Bak BLV, Glud JA, J S, Christensen ET (2017) A user programmed cohesive zone finite element for ansys mechanical. Eng Frac Mech 38(11):1072–1089

McGugan M, Pereira G, Sørensen BF, Toftegaard H, Branner K (2015) Damage tolerance and structural monitoring for wind turbine blades. Philosophical Transactions of the Royal Society A 373:2014007

Mi U, Crisfield M, Davies G (1998) Progressive delamination using interface elements. Journal of Composite Materials 32:1246–1272

Mikkelsen LP (2016) A simplified model predicting the weight of the load carrying beam in a wind turbine blade. IOP Conf Ser: Mater Sci Eng 139:012038

Millán JS, Armendáriz I (2015) Delamination and Debonding Growth in Composite Structures. [In: Riccio A. (eds) Damage Growth in Aerospace Composites. Springer Aerospace Technology. Springer, Cham.

Miner MA (1945) Cumulative damage in fatigue. Trans ASME, J Appl Mech 67:p. A159

Moës N, Belytschko T (2002) Extended finite element method for cohesive crack growth. Engineering Fracture Mechanics 69:813–833

Moës N, Dolbow J, Belytschko T (1999) A finite element method for crack growth without remeshing. International Journal for Numerical Methods in Engineering 46:131–150

Nghiem A, Pineda I (2017) Wind energy in Europe: Scenarios for 2030. Tech. rep., In: Tardieu P. (eds), Wind Europe, September 2017, windeurope.org

Ortiz M, Pandolfi A (1999) Finite-deformation irreversible cohesive elements for three-dimensional crack-propagation analysis. Int J Numer Meth Eng 44(9):1267–1282

Pagano NJ, Schoeppner GA (2000) Delamination of polymer matrix composites: Problems and assessment. Comprehensive Composite Materials 2:433–528

Palmgren A (1924) Durability of ball bearings. ZDVDI, Vol 68, No 14 p p.339

Paris P, Erdogan F (1963) A critical analysis of crack propagation laws. J Basic Eng 85 (4):528–533

Paris P, Gomez M, Anderson W (1961) A rational analytic theory of fatigue. The Trend in Engineering 13:9–14

Park K, Paulino GH (2011) Cohesive zone models: A critical review of traction-separation relationships across fracture surfaces. Applied Mechanics Reviews 64:060802

Pereira FAM, Morais JJL, de Moura MFSF, Dourado N, Dias MIR (2012) Evaluation of bone cohesive laws using an inverse method applied to the dcb test. Engineering Fracture Mechanics 96:724–736

Pereira FAM, de Moura MFSF, Dourado N, Morais JJL, Xavier J, Dias MIR (2017) Direct and inverse methods applied to the determination of mode i cohesive law of bovine cortical bone using the dcb test. International Journal of Solids and Structures 128:210–220

Pereira FAM, de Moura MFSF, Dourado N, Morais JJL, Xavier J, Dias MIR (2018) Determination of mode ii cohesive law of bovine cortical bone using direct and inverse methods. International Journal of Mechanical Sciences 138-139:448–456

Petersson PE (1981) Crack growth and development of fracture zones in plain concrete and similar materials. Tech. rep., Report TVBM-100, Div. of Building Materials, Lund Institute of Technology, Sweden)

Rans C, Alderliesten R, Benedictus R (2011) Misinterpreting the results: How similitude can improve our understanding of fatigue delamination growth. Composites Science and Technology 71:230–238

Rice JR (1968) A path independent integral and the approximate analysis of strain concentrations by notches and cracks. Journal of Applied Mechanics 35:379

Rigby RH, Aliabadi MH (1998) Decomposition of the mixed mode j-integral - revisited. Int J Solids Struct 35(17):2073–99

Rosling H (2013) Don't Panic - The Facts About Population. Tech. rep., Gapminder.org, producer: Wingspan Productions

Rybicki EF, Kanninen MF (1977) A finite element calculation of stress intensity factors by a modified crack closure integral. Engineering Fracture Mechanics 9:931–938

Sarfaraz R, Vassilopoulos AP, Keller T (2013a) Block loading fatigue of adhesively bonded pultruded gfrp joints. International Journal of Fatigue 49:40–49

Sarfaraz R, Vassilopoulos AP, Keller T (2013b) Variable amplitude fatigue of adhesively-bonded pultruded gfrp joints. International Journal of Fatigue 55:22–32

Sarrado C, Turon A, Renart J, Urresti I (2012) Assessment of energy dissipation during mixed-mode delamination growth using cohesive zone models. Composites: Part A 43:2128–2136

Schaff JR, Davidson BD (1997a) Life prediction methodology for composite structures part i - constant amplitude and two-stress level fatigue. J Composite Mater 31 (2):128–157

Schaff JR, Davidson BD (1997b) Life prediction methodology for composite structures part ii - spectrum fatigue. J Composite Mater 31 (2):158–181

Schijve J (2009) Fatigue of Structures and Materials. Springer

Schütz D, Lowak H, de Jonge JB, Schijve J (1973) A standardised load sequence for flight simulation tests on transport aircraft wing structures. Tech. rep., LBF-Report FB-106, NLR-Report TR 73

Schütz D, Klätschke H, Steinhilber H, Heuler P, Schütz W (1990) Standardized load sequences for car wheel suspension components. Car loading standard - CARLOS. Final report. Tech. rep., Fraunhofer-Institut für Betriebsfestigkeit (LBF), Darmstadt, Industrieanlagen-Betriebsgesellschaft mbH (IABG), Ottobrunn, LBF-Report No. FB-191

Segurado J, Llorca A (2004) A new three-dimensional interface finite element to simulate fracture in composites. International Journal of Solids and Structures 41 (11-12):2977–2993

Shen B, Paulino G (2011) Direct extraction of cohesive fracture properties from digital image correlation: A hybdid inverse technique. Experimental Mechanics 51:143–163

Shen B, Stanciulescu I, Paulino G (2010) Inverse computation of cohesive fracture properties from displacement fields. Taylor & Francis 18 No. 8:1103–1128

Sih GC, Paris PC, Irwin GR (1965) On cracks in rectilinearly anisotropic bodies. International Journal of Fracture Mechanics 1:189–203

Soerensen BF, K GE, Oestergaard RC, Goutianos S (2008) Micromechanical model of cross-over fibre bridging - prediction of mixed mode bridging laws. Mechanics of Materials 40:220–234

Sorensen L, Botsis J, Gmür T, Cugnoni J (2007) Delamination detection and characterisation of bridging tractions using long fbg optical sensors. Composites: Part A 38:2087–2096

Sorensen L, Botsis J, Gmür T, Humbert L (2008) Bridging tractions in mode i delamination: Measurements and simulations. Composites Science and Technology 68:2350–2358

Spearing SM, Evans AG (1992) The role of fiber bridging in delamination resistance of fiber-reinforced composites. Acta Metall Mater 40:2191–2199

Sørensen BF (2016) Delamination fractures in composite materials. [In: Talreja A. and Varna J. (eds) Modeling Damage, Fatigue and Failure of Composite Materials. Woodhead Publishing Series in Composites Science and Engineering: Number 65.

Sørensen BF, Jacobsen TK (1998) Large-scale bridging in composites: R-curves and bridging laws. Composites part A 29A:1443–1451

Sørensen BF, Jacobsen TK (2000) Crack growth in composites applicability of r-curves and bridging laws. Plastics, Rubber and Composites 29:3:119–133

Sørensen BF, Jacobsen TK (2003) Determination of cohesive laws by the j integral approach. Engineering Fracture Mechanics 70:1841–1858

Sørensen BF, Kirkegaard P (2006) Determination of mixed mode cohesive laws. Engineering Fracture Mechanics 73:2642–2661

Sørensen BF, Jørgensen E, Debel CP, Jensen FM, Jacobsen TK, Halling K (2004) Improved design of large wind turbine blade of fibre composites based on studies of scale effects (Phase 1). Summary report. Tech. rep., Risø National Laboratory. Denmark. Forskningscenter Risoe. Risoe-R, No. 1390 (EN)

Sørensen BF, Gamstedt EK, Østergaard RC, Goutianos S (2008) Micromechanical model of cross-over fibre bridging - prediction of mixed mode bridging laws. Mechanics of Materials 40:220–234

Sun CT, Jin ZH (2012) Fracture Mechanics. Elsevier Inc.

Suo Z, Bao G, Fan B (1992) Delamination r-curve phenomena due to damage. J Mech Phys Solids 40:1–16

Tabiei A, Zhang W (2018) Composite laminate delamination simulation and experiment: A review of recent development. Applied Mechanics Review 70 (3):030801

Talreja R (2000) Fagitue damage evolution in composites - a new way forward in modeling. In: Session 9: Analysis Methods, Second International Conference on Fatigue of Composites

Talreja R, Varna J (2016) Modeling Damage, Fatigue and Failure of Composite Materials. Woodhead Publishing

Tamuzs V, Tarasovs S, Vilks U (2001) Progressive delamination and fiber bridging modelling in double cantilever beam composite specimens. Engineering Fracture Mechanics 68:513–525

Turon A, Camanho PP, Costa J, Dávila CG (2006) A damage model for the simulation of delamination in advanced composites under variable-mode loading. Mech Mater 38(11):1072–1089

Turon A, Camanho PP, Costa J, Renart J (2010) Accurate simulation of delamination growth under mixed-mode loading using cohesive elements: Definition of interlaminar strengths and elastic stiffness. Composite Structures 92:1857–1864

Tvergaard V, Hutchinson JM (1992) The relation between crack growth resistance and fracture process parameters in elastic-plastic solids. Journal of the Mechanics and Physics of Solids 40(6):1377–1397

United Nations (2019) World population prospects 2019: Highlights. Tech. rep., Department of Economic and Social Affairs, Population Division. ST/ESA/SER.A/423

Van Paepegem W, Degrieck J (2002) Effects of load sequence and block loading on the fatigue response of fiber-reinforced composites. Mechanics of Advanced Materials and Structures 9(1):19–35

Vassilopoulos AP (2015) Block and variable amplitude fatigue and fracture behavior of adhesively-bonded composite structural joints, Fatigue and Fracture of Adhesively-bonded Composite Joints, vol Chapt. 9. Elsevier Inc

Vestas (2021) V236-15.0 MW at a glance. `https://www.vestas.com/en/products/offshore%20platforms/v236_15_mw#!technical-specifications`, online; accessed April 2021

Whitney JM (1989) Experimental characterization of delamination fracture. [In: Pagano N. J. (eds) Interlaminar response of composite materials. Elsevier.

WindEurope (2021) Wind energy in Europe 2020 Statistics and the outlook for 2021-2025. `https://windeurope.org/intelligence-platform/product/wind-energy-in-europe-in-2020-trends-and-statistics/`, online; accessed April 2021

Wittrup S (2021) Gigantiske møller varsler gennembrud for havvind. `https://ing.dk/artikel/gigantiske-moeller-varsler-gennembrud-havvind-245587`, online; accessed April 2021

Xu XP, Needleman A (1994) Numerical simulations of fast crack growth in brittle solids. Journal of the Mechanics and Physics of Solids 42(9):1397–1434

Xu Y, Guo Y, Liang L, Liu Y, Wang X (2017) A unified cohesive zone model for simulating adhesive failure of composite structures and its parameter identification. Composite Structures 182:555–565

Yang JN, Jones DL (1981) Load sequence effects on the fatigue of unnotched composite materials. Fatigue of Fibrous Composite Materials, ASTM STP 723:213–232

Yao L, Alderliesten R, Zhao M, Benedictus R (2014) Bridging effect on mode i fatigue delamination behavior in composite laminates. Composites: Part A 63:103–109

Yao L, Alderliesten R, Benedictus R (2016a) The effect of fiber bridging on the paris relation for mode i fatigue delamination growth in composites. Composite Structures 140:125–135

Yao L, Sun Y, Alderliesten RC, Benedictus R (2016b) Fatigue delamination growth behavior in composite materials under block loading. 31st Annual Technical Conference of the American Society for Composites: Williamsburg, Virginia, USA, 19-22 September 2:1347–1358

Yao L, Sun Y, Alderliesten RC, Benedictus R, Zhao M (2017a) Fibre bridging effect on the paris relation for mode i fatigue delamination growth in composites with consideration of interface configuration. Composite Structures 159:471–478

Yao L, Sun Y, Guo L, Alderliesten RC, Benedictus R, Zhao M, Jia L (2017b) Fibre bridging effect on the paris relation of mode i fatigue delamination in composite laminates with different thickness. International Journal of Fatigue 103:196–206

Ye L (1988) Role of matrix resin in delamination onset and growth in composite laminates. Composites Science and Technology 33:257–277

Zehnder AT (2012) Fracture Mechanics, vol 62. [In: Pfeiffer F. and Wriggers, P. (eds) Lecture Notes in Applied and Computational Mechanics. Springer.